Acknowledgments

This work was supported in part by Grants-in-Aid for Scientific Research (No. 16209056, No. 17209065, No. 17390560, No. 17390561 and No. 18890107) and the 21st Century COE entitled "Origination of Frontier BioDentistry" at Osaka University Graduate School of Dentistry supported by the Ministry of Education, Culture, Sports, Science and Technology.

Literature Cited

Aeschlimann D, Wetterwald A, Fleisch H, Paulsson M. 1993. Expression of tissue transglutaminase in skeletal tissues correlates with events of terminal differentiation of chondrocytes. J Cell Biol 120:1461–1470.

Aeschlimann D, Kaupp O, Paulsson M. 1995. Transglutaminase-catalyzed matrix cross-linking in differentiating cartilage: Identification of osteonectin as a major glutaminyl substrate. J Cell Biol 129:881–892.

Agnholt J, Kelsen J, Schack L, Hvas CL, Dahlerup JF, Sørensen ES. 2007. Osteopontin, a protein with cytokine-like properties, is associated with inflammation in Crohn's disease. Scand J Immunol 65:453–460.

Ashkar S, Weber GF, Panoutsakopoulou V, Sanchirico ME, Jansson M, Zawaideh S, Rittling SR, Denhardt DT, Glimcher MJ, Cantor H. 2000. Eta-1 (osteopontin): An early component of type-1 (cell-mediated) immunity. Science 287:860–864.

Beck GRJ, Moran E, Knecht N. 2003. Inorganic phosphate regulates multiple genes during osteoblast differentiation, including Nrf2. Exp Cell Res 288:288–300.

Bellows CG, Heersche JN, Aubin JE. 1992. Inorganic phosphate added exogenously or released from beta-glycerophosphate initiates mineralization of osteoid nodules in vitro. Bone Miner 17:15–29.

Bendeck MP, Irvin C, Reidy M, Smith L, Mulholland D, Horton M, Giachelli CM. 2000. Smooth muscle cell matrix metalloproteinase production is stimulated via alpha(v)beta(3) integrin. Arterioscler Thromb Vasc Biol 20:1467–1472.

Bessey OA, Lowry OH. 1946. A method for rapid determination of alkaline phosphatase with five cubic millimeters of serum. J Biol Chem 164:321–329.

Boskey AL, Maresca M, Ullrich W, Doty SB, Butler WT, Prince CW. 1993. Osteopontin-hydroxyapatite interactions in vitro: Inhibition of hydroxyapatite formation and growth in a gelatin-gel. Bone Miner 22:147–159.

Castellone MD, Celetti A, Guarino V, Cirafici AM, Basolo F, Giannini R, Medico E, Kruhoffer M, Orntoft TF, Curcio F, Fusco A, Melillo RM, Santoro M. 2004. Autocrine stimulation by osteopontin plays a pivotal role in the expression of the mitogenic and invasive phenotype of RET/PTC-transformed thyroid cells. Oncogene 23:2188–2196.

Chellaiah MA, Hruska KA. 2003. The integrin alpha(v)beta(3) and CD44 regulate the actions of osteopontin on osteoclast motility. Calcif Tissue Int 72:197–205.

Chung CH, Golub EE, Forbes ETT, Shapiro IM. 1992. Mechanism of action of beta-glycerophosphate on bone cell mineralization. Calcif Tissue Int 51:305–311.

Dahl LK. 1952. A simple and sensitive histochemical method for calcium. Proc Soc Exp Biol Med 80:474–479.

Debiais F, Lefevre G, Lemonnier J, Le Mee S, Lasmoles F, Mascarelli F, Marie PJ. 2004. Fibroblast growth factor-2 induces osteoblast survival through a phosphatidylinositol 3-kinase-dependent, -beta-catenin-independent signaling pathway. Exp Cell Res 297:235–246.

Denhardt DT, Guo XJ. 1993. Osteopontin: A protein with diverse functions. FASEB J 7:1475–1482.

Denhardt DT, Noda M. 1998. Osteopontin expression and function: Role in bone remodeling. J Cell Biochem Suppl 30–31:92–102 (Review).

Denhardt DT, Giachelli CM, Rittling SR. 2001a. Role of osteopontin in cellular signaling and toxicant injury. Annu Rev Pharmacol Toxicol 41:723–749.

Denhardt DT, Noda M, O'Regan AW, Pavlin D, Berman JS. 2001b. Osteopontin as a means to cope with environmental insults: Regulation of inflammation, tissue remodeling, and cell survival. J Clin Invest 107:1055–1061.

Foster BL, Nociti FHJ, Swanson EC, Matsa-Dunn D, Berry JE, Cupp CJ, Zhang P, Somerman MJ. 2006. Regulation of cementoblast gene expression by inorganic phosphate in vitro. Calcif Tissue Int 78:103–112.

Giachelli CM, Pichler R, Lombardi D, Denhardt DT, Alpers CE, Schwartz SM, Johnson RJ. 1994. Osteopontin expression in angiotensin II-induced tubulointerstitial nephritis. Kidney Int 45:515–524.

Glimcher MJ. 1989. Mechanism of calcification: Role of collagen fibrils and collagen-phosphoprotein complexes in vitro and in vivo. Anat Rec 224:139–153.

Guo H, Cai CQ, Schroeder RA, Kuo PC. 2001. Osteopontin is a negative feedback regulator of nitric oxide synthesis in murine macrophages. J Immunol 166:1079–1086.

Hakki SS, Nohutcu RM, Hakki EE, Berry JE, Akkaya MS, Somerman MJ. 2005. Dexamethasone and basic-fibroblast growth factor regulate markers of mineralization in cementoblasts in vitro. J Periodontol 76:1550–1558.

Hashimoto M, Koda M, Ino H, Murakami M, Yamazaki M, Moriya H. 2003. Upregulation of osteopontin expression in rat spinal cord microglia after traumatic injury. J Neurotrauma 20:287–296.

Heath DJ, Downes S, Verderio E, Griffin M. 2001. Characterization of tissue transglutaminase in human osteoblast-like cells. J Bone Miner Res 16:1477–1485.

Hijiya N, Setoguchi M, Matsuura K, Higuchi Y, Akizuki S, Yamamoto S. 1994. Cloning and characterization of the human osteopontin gene and its promoter. Biochem J 303:255–262.

Ishijima M, Tsuji K, Rittling SR, Yamashita T, Kurosawa H, Denhardt DT, Nifuji A, Ezura Y, Noda M. 2007. Osteopontin is required for mechanical stress-dependent signals to bone marrow cells. J Endocrinol 193:235–243.

Jono S, Peinado C, Giachelli CM. 2000. Phosphorylation of osteopontin is required for inhibition of vascular smooth muscle cell calcification. J Biol Chem 275:20197–20203.

Kaartinen MT, Pirhonen A, Linnala-Kankkunen A, Maenpaa PH. 1999. Cross-linking of osteopontin by tissue transglutaminase increases its collagen binding properties. J Biol Chem 274:1729–1735.

Khan SA, Lopez-Chua CA, Zhang J, Fisher LW, Sorensen ES, Denhardt DT. 2002. Soluble osteopontin inhibits apoptosis of adherent endothelial cells deprived of growth factors. J Cell Biochem 85:728–736.

Kim HJ, Lee MH, Park HS, Park MH, Lee SW, Kim SY, Choi JY, Shin HI, Kim HJ, Ryoo HM. 2003. Erk pathway and activator protein 1 play crucial roles in FGF2-stimulated premature cranial suture closure. Dev Dyn 227:335–346.

Labarca C, Paigen K. 1980. A simple, rapid, and sensitive DNA assay procedure. Anal Biochem 102:344–352.

Lao M, Marino V, Bartold PM. 2006. Immunohistochemical study of bone sialoprotein and osteopontin in healthy and diseased root surfaces. J Periodontol 77:1665–1673.

Leali D, Dell'Era P, Stabile H, Sennino B, Chambers AF, Naldini A, Sozzani S, Nico B, Ribatti D, Presta M. 2003. Osteopontin (Eta-1) and fibroblast growth factor-2 cross-talk in angiogenesis. J Immunol 171:1085–1093.

Li G, Chen YF, Kelpke SS, Oparil S, Thompson JA. 2000. Estrogen attenuates integrin-beta(3)-dependent adventitial fibroblast migration after inhibition of osteopontin production in vascular smooth muscle cells. Circulation 101:2949–2955.

Liaw L, Almeida M, Hart CE, Schwartz SM, Giachelli CM. 1994. Osteopontin promotes vascular cell adhesion and spreading and is chemotactic for smooth muscle cells in vitro. Circ Res 74:214–224.

Liaw L, Birk DE, Ballas CB, Whitsitt JS, Davidson JM, Hogan BL. 1998. Altered wound healing in mice lacking a functional osteopontin gene (spp1). J Clin Invest 101:1468–1478.

Lin YH, Yang-Yen HF. 2001. The osteopontin-CD44 survival signal involves activation of the phosphatidylinositol 3-kinase/Akt signaling pathway. J Biol Chem 276:46024–46030.

Lin YH, Huang CJ, Chao JR, Chen ST, Lee SF, Yen JJ, Yang-Yen HF. 2000. Coupling of osteopontin and its cell surface receptor CD44 to the cell survival response elicited by interleukin-3 or granulocyte-macrophage colony-stimulating factor. Mol Cell Biol 20:2734–2742.

MacNeil RL, Berry J, D'Errico J, Strayhorn C, Piotrowski B, Somerman MJ. 1995a. Role of two mineral-associated adhesion molecules, osteopontin and bone sialoprotein, during cementogenesis. Connect Tissue Res 33:1–7 (Review).

MacNeil RL, Berry J, D'Errico J, Strayhorn C, Somerman MJ. 1995b. Localization and expression of osteopontin in mineralized and nonmineralized tissues of the periodontium. Ann N Y Acad Sci 760:166–176 (Review).

McKee MD, Nanci A. 1996. Secretion of Osteopontin by macrophages and its accumulation at tissue surfaces during wound healing in mineralized tissues: A potential requirement for macrophage adhesion and phagocytosis. Anat Rec 245:394–409.

Mukherjee BB, Nemir M, Beninati S, Cordella-Miele E, Singh K, Chackalaparampil I, Shanmugam V, DeVouge MW, Mukherjee AB. 1995. Interaction of osteopontin with fibronectin and other extracellular matrix molecules. Ann N Y Acad Sci 21:201–212.

Murakami S, Takayama S, Ikezawa K, Shimabukuro Y, Kitamura M, Nozaki T, Terashima A, Asano T, Okada H. 1999. Regeneration of periodontal tissues by basic fibroblast growth factor. J Periodontal Res 34:425–430.

Murakami S, Takayama S, Kitamura M, Shimabukuro Y, Yanagi K, Ikezawa K, Saho T, Nozaki T, Okada H. 2003. Recombinant human basic fibroblast growth factor (bFGF) stimulates periodontal regeneration in class II furcation defects created in beagle dogs. J Periodontal Res 38:97–103.

Murry CE, Giachelli CM, Schwartz SM, Vracko R. 1994. Macrophages express osteopontin during repair of myocardial necrosis. Am J Pathol 145:1450–1462.

Naldini A, Leali D, Pucci A, Morena E, Carraro F, Nico B, Ribatti D, Presta M. 2006. IL-1beta mediates the proangiogenic activity of osteopontin-activated human monocytes. J Immunol 177:4267–4270.

Nau GJ, Guilfoile P, Chupp GL, Berman JS, Kim SJ, Kornfeld H, Young RA. 1997. A chemoattractant cytokine associated with granulomas in tuberculosis and silicosis. Proc Natl Acad Sci USA 94:6414–6419.

Nau GJ, Chupp GL, Emile JF, Jouanguy E, Berman JS, Casanova JL, Young RA. 2000. Osteopontin expression correlates with clinical outcome in patients with mycobacterial infection. Am J Pathol 157:37–42.

Noiri E, Dickman K, Miller F, Romanov G, Romanov VI, Shaw R, Chambers AF, Rittling SR, Denhardt DT, Goligorsky MS. 1999. Reduced tolerance to acute renal ischemia in mice with a targeted disruption of the osteopontin gene. Kidney Int 56:74–82.

O'Brien ER, Garvin MR, Stewart DK, Hinohara T, Simpson JB, Schwartz SM, Giachelli CM. 1994. Osteopontin is synthesized by macrophage, smooth muscle, and endothelial cells in primary and restenotic human coronary atherosclerotic plaques. Arterioscler Thromb 14:1648–1656.

Ophascharoensuk V, Giachelli CM, Gordon K, Hughes J, Pichler R, Brown P, Liaw L, Schmidt R, Shankland SJ, Alpers CE, Couser WG, Johnson RJ. 1999. Obstructive uropathy in the mouse: Role of osteopontin in interstitial fibrosis and apoptosis. Kidney Int 56:571–580.

O'Regan A, Berman JS. 2000. Osteopontin: A key cytokine in cell-mediated and granulomatous inflammation. Int J Exp Pathol 81:373–390.

O'Regan AW, Chupp GL, Lowry JA, Goetschkes M, Mulligan N, Berman JS. 1999. Osteopontin is associated with T cells in sarcoid granulomas and has T cell adhesive and cytokine-like properties in vitro. J Immunol 162:1024–1031.

Pampena DA, Robertson KA, Litvinova O, Lajoie G, Goldberg HA, Hunter GK. 2004. Inhibition of hydroxyapatite formation by osteopontin phosphopeptides. Biochem J 378:1083–1087.

Patarca R, Freeman GJ, Singh RP, Wei FY, Durfee T, Blattner F, Regnier DC, Kozak CA, Mock BA, Morse HCI, Jerrells TR, Cantor H. 1989. Structural and functional studies of the early T lymphocyte activation 1 (Eta-1) gene. Definition of a novel T cell-dependent response associated with genetic resistance to bacterial infection. J Exp Med 170:145–161.

Persy VP, Verhulst A, Ysebaert DK, De Greef KE, De Broe ME. 2003. Reduced postischemic macrophage infiltration and interstitial fibrosis in osteopontin knockout mice. Kidney Int 63:543–553.

Rajamannan NM, Nealis TB, Subramaniam M, Pandya S, Stock SR, Ignatiev CI, Sebo TJ, Rosengart TK, Edwards WD, McCarthy PM, Bonow RO, Spelsberg TC. 2005. Calcified rheumatic valve neoangiogenesis is associated with vascular endothelial growth factor expression and osteoblast-like bone formation. Circulation 111:3296–3301.

Rittling SR, Chen Y, Feng F, Wu Y. 2002. Tumor-derived osteopontin is soluble, not matrix associated. J Biol Chem 277:9175–9182.

Rogers SA, Padanilam BJ, Hruska KA, Giachelli CM, Hammerman MR. 1997. Metanephric osteopontin regulates nephrogenesis in vitro. Am J Physiol 272:F469–F476.

Rollo EE, Laskin DL, Denhardt DT. 1996. Osteopontin inhibits nitric oxide production and cytotoxicity by activated R AW264.7 macrophages. J Leukoc Biol 60:397.

Saavedra RA. 1994. The roles of autophosphorylation and phosphorylation in the life of osteopontin. Bioessays 16:913–918.

Scatena M, Almeida M, Chaisson ML, Fausto N, Nicosia RF, Giachelli CM. 1998. NF-kappaB mediates alphavbeta3 integrin-induced endothelial cell survival. J Cell Biol 141:1083–1093.

Senger DR, Asch BB, Smith BD, Perruzzi CA, Dvorak HF. 1983. A secreted phosphoprotein marker for neoplastic transformation of both epithelial and fibroblastic cells. Nature 302:714–715.

Senger DR, Ledbetter SR, Claffey KP, Papadopoulos-Sergiou A, Peruzzi CA, Detmar M. 1996. Stimulation of endothelial cell migration by vascular permeability factor/vascular endothelial growth factor through cooperative mechanisms involving the alphavbeta3 integrin, osteopontin, and thrombin. Am J Pathol 149:293–305.

Seo BM, Miura M, Gronthos S, Bartold PM, Batouli S, Brahim J, Young M, Robey PG, Wang CY, Shi S. 2004. Investigation of multipotent postnatal stem cells from human periodontal ligament. Lancet 364:149–155.

Shimabukuro Y, Ichikawa T, Takayama S, Yamada S, Takedachi M, Terakura M, Hashikawa T, Murakami S. 2005. Fibroblast growth factor-2 regulates the synthesis of hyaluronan by human periodontal ligament cells. J Cell Physiol 203:557–563.

Singh K, DeVouge MW, Mukherjee BB. 1990. Physiological properties and differential glycosylation of phosphorylated and nonphosphorylated forms of osteopontin secreted by normal rat kidney cells. J Biol Chem 265:18696–18701.

Sorensen ES, Petersen TE. 1995. Phosphorylation, glycosylation, and transglutaminase sites in bovine osteopontin. Ann N Y Acad Sci 760:363–366.

Srivatsa SS, Harrity PJ, Maercklein PB, Kleppe L, Veinot J, Edwards WD, Johnson CM, Fitzpatrick LA. 1997. Increased cellular expression of matrix proteins that regulate mineralization is associated with calcification of native human and porcine xenograft bioprosthetic heart valves. J Clin Invest 99:996–1009.

Takahashi F, Takahashi K, Okazaki T, Maeda K, Ienaga H, Maeda M, Kon S, Uede T, Fukuchi Y. 2001. Role of osteopontin in the pathogenesis of bleomycin-induced pulmonary fibrosis. Am J Respir Cell Mol Biol 24:264–271.

Takayama S, Murakami S, Miki Y, Ikezawa K, Tanaka S, Terashima A, Asano T, Okada H. 1997. Effects of basic fibroblast growth factor on human periodontal ligament cells. J Periodontal Res 32:667–675.

Takayama S, Murakami S, Shimabukuro Y, Kitamura M, Okada H. 2001. Periodontal regeneration by FGF-2 (bFGF) in primate models. J Dent Res 80:2075–2079.

Weintraub AS, Schnapp LM, Lin X, Taubman MB. 2000. Osteopontin deficiency in rat vascular smooth muscle cells is associated with an inability to adhere to collagen and increased apoptosis. Lab Invest 80:1603–1615.

Xiao G, Jiang D, Gopalakrishnan R, Franceschi RT. 2002. Fibroblast growth factor 2 induction of the osteocalcin gene requires MAPK activity and phosphorylation of the osteoblast transcription factor, Cbfa1/Runx2. J Biol Chem 277:36181–36187.

Yamada S, Tomoeda M, Ozawa Y, Yoneda S, Terashima Y, Ikezawa K, Ikegawa S, Saito M, Toyosawa S, Murakami S. 2007. PLAP-1/Asporin: A novel negative regulator of periodontal ligament mineralization. J Biol Chem 282:23070–23080.

Zohar R, Lee W, Arora P, Cheifetz S, McCulloch C, Sodek J. 1997. Single cell analysis of intracellular osteopontin in osteogenic cultures of fetal rat calvarial cells. J Cell Physiol 170:88–100.

Zohar R, Suzuki N, Suzuki K, Arora P, Glogauer M, McCulloch CA, Sodek J. 2000. Intracellular osteopontin is an integral component of the CD44-ERM complex involved in cell migration. J Cell Physiol 184:118–130.

CD73-Generated Adenosine Restricts Lymphocyte Migration into Draining Lymph Nodes[1]

Masahide Takedachi,*‡ Dongfeng Qu,* Yukihiko Ebisuno,[2†] Hiroyuki Oohara,‡ Michelle L. Joachims,* Stephanie T. McGee,* Emiko Maeda,* Rodger P. McEver,† Toshiyuki Tanaka,§ Masayuki Miyasaka,¶ Shinya Murakami,‡ Thomas Krahn,‖ Michael R. Blackburn,# and Linda F. Thompson[3]*

After an inflammatory stimulus, lymphocyte migration into draining lymph nodes increases dramatically to facilitate the encounter of naive T cells with Ag-loaded dendritic cells. In this study, we show that CD73 (ecto-5′-nucleotidase) plays an important role in regulating this process. CD73 produces adenosine from AMP and is expressed on high endothelial venules (HEV) and subsets of lymphocytes. *Cd73*$^{-/-}$ mice have normal sized lymphoid organs in the steady state, but 1.5-fold larger draining lymph nodes and 2.5-fold increased rates of L-selectin-dependent lymphocyte migration from the blood through HEV compared with wild-type mice 24 h after LPS administration. Migration rates of *cd73*$^{+/+}$ and *cd73*$^{-/-}$ lymphocytes into lymph nodes of wild-type mice are equal, suggesting that it is CD73 on HEV that regulates lymphocyte migration into draining lymph nodes. The A_{2B} receptor is a likely target of CD73-generated adenosine, because it is the only adenosine receptor expressed on the HEV-like cell line KOP2.16 and it is up-regulated by TNF-α. Furthermore, increased lymphocyte migration into draining lymph nodes of *cd73*$^{-/-}$ mice is largely normalized by pretreatment with the selective A_{2B} receptor agonist BAY 60-6583. Adenosine receptor signaling to restrict lymphocyte migration across HEV may be an important mechanism to control the magnitude of an inflammatory response. *The Journal of Immunology*, **2008, 180: 6288–6296.**

Lymphocyte circulation from the bloodstream to lymph nodes is necessary for immune homeostasis (reconnaissance) under normal physiological conditions and for immune responses against exogenous Ags. This trafficking requires coordinated action of adhesion molecules, chemokines, and chemokine receptors expressed on lymphocytes and high endothelial venules (HEV)[4] (reviewed in Refs. 1 and 2). The interaction of L-selectin with peripheral lymph node addressins (PNAd) initiates lymphocyte tethering and rolling on HEV (3). Chemokine receptor signaling activates the integrin LFA-1 on lymphocytes and induces stable adhesion via binding to ICAM-1 on HEV (4, 5), which is followed by transmigration. The importance of each molecule associated with the entrance of lymphocytes into lymph nodes through HEV has been shown by decreases in lymph node cellularity and defective immune responses in gene-targeted mice (6–10).

TLR signaling activates innate immune responses (reviewed in Ref. 11) in part by inducing APC maturation and recruitment to lymphoid organs via the afferent lymphatics (12, 13). Furthermore, recent reports showed that inflammation induced by a TLR4 or TLR9 agonist controlled naive lymphocyte recirculation in an Ag-independent manner, resulting in an increase in the number of naive lymphocytes in the draining lymph node and an increase in the efficiency of lymphocyte-APC encounters (14). TLR-dependent lymph node hypertrophy was proposed to require vascular growth and arteriole thickening. Although these changes needed at least a few days before they were detectible (14, 15), lymph node growth began within 24 h after a stimulus, implying the existence of other mechanisms that contribute to lymph node swelling. In this study, we present data to show that adenosine (Ado) receptor (AR) signaling, mediated by CD73-generated Ado, plays an important role in regulating early migration of lymphocytes to draining lymph nodes.

CD73 is a 70-kDa GPI-anchored protein with ecto-5′ nucleotidase enzyme activity that catalyzes the dephosphorylation of extracellular nucleoside monophosphates such as AMP to nucleosides such as Ado (16). Extracellular Ado can engage four subtypes of ubiquitously expressed AR (A_1AR, A_{2A}AR, A_{2B}AR, and A_3AR) to modulate a wide array of physiological responses, including vascular tone, neurotransmission, cytokine production, heart rate, and adaptation to hypoxia (reviewed in Ref. 17). In addition to being generated

*Immunobiology and Cancer Program and †Cardiovascular Biology Program, Oklahoma Medical Research Foundation, Oklahoma City, OK 73104; ‡Department of Periodontology, Division of Oral Biology and Disease Control, Osaka University Graduate School of Dentistry, Osaka, Japan; §Laboratory of Immunobiology, Hyogo University of Health Sciences, Kobe, Japan; ¶Laboratory of Molecular and Cellular Recognition, Osaka University Graduate School of Medicine, Osaka, Japan; ‖Bayer HealthCare Wuppertal, Germany; and #Department of Biochemistry and Molecular Biology, University of Texas Medical School, Houston, TX 77030

Received for publication April 23, 2007. Accepted for publication March 3, 2008.

The costs of publication of this article were defrayed in part by the payment of page charges. This article must therefore be hereby marked *advertisement* in accordance with 18 U.S.C. Section 1734 solely to indicate this fact.

[1] This work was supported by National Institutes of Health Grants AI18220 (to L.F.T.), P01 HL085607 (to R.P.M.), and AI43472 (to M.R.B.), and was part of the 21st Century Center of Excellence entitled "Origination of Frontier BioDentistry" at Osaka University Graduate School of Dentistry supported by the Ministry of Education, Culture, Sports, Science, and Technology. L.F.T. holds the Putnam City Schools Distinguished Chair in Cancer Research. R.P.M. holds the Eli Lilly Distinguished Chair in Biomedical Research.

[2] Current address: Department of Molecular Genetics, Institute of Biomedical Science, Kansai Medical University, Osaka, Japan 570-8506.

[3] Address correspondence and reprint requests to Dr. Linda F. Thompson, Oklahoma Medical Research Foundation, 825 Northeast 13th Street, Oklahoma City, OK 73104. E-mail address: Linda-Thompson@omrf.org

[4] Abbreviations used in this paper: HEV, high endothelial venule; Ado, adenosine; AR, Ado receptor; CMFDA, 5-chloromethylfluorescein diacetate; CMTMR, 5-and 6-(4-chloromethylbenzoylamino)tetramethylrhodamine; DC, dendritic cell; PEG, polyethylene glycol; PNAd, peripheral lymph node addressin.

intracellularly through the action of cytoplasmic nucleotidases and then exported via nucleoside transporters. Extracellular Ado has a very short $t_{1/2}$, because it is efficiently taken up into the cytoplasm, where it can be phosphorylated to AMP or degraded to inosine by Ado deaminase. In humans, Ado deaminase can be localized to the cell surface via binding to CD26 (18, 19), giving it the potential to inhibit AR signaling through deamination of extracellular Ado (20). Mice deficient in the expression of each AR have been engineered and characterized (21–25). Each strain has a variety of interesting phenotypes, revealing the diverse consequences of AR signaling. However, the mechanism by which extracellular Ado levels are regulated to modulate AR engagement in vivo is not fully understood.

Ado is a well-known anti-inflammatory mediator (26). Recent studies clearly showed that CD73 makes a major contribution to the generation of extracellular Ado in a number of physiologically relevant experimental models and plays a critical role in host defense systems. For example, CD73 attenuates hypoxia-induced vascular leakage, FMLP-stimulated neutrophil adhesion to endothelial cells, and neutrophil accumulation in tissues (27–29). Furthermore, *cd73*-deficient mice are susceptible to vascular inflammation and neointima formation due to decreased concentrations of endogenous Ado (30). CD73 deficiency increases VCAM-1 expression on endothelial cells isolated from carotid arteries through NF-κB activation; however, ICAM-1 expression is unchanged. This proinflammatory phenotype of *cd73*-deficient endothelium causes the arrest of monocytes and exacerbates wire-induced injury.

These observations demonstrated a crucial role for CD73-generated Ado in the interaction of myeloid cells with vascular endothelium. However, the in vivo function of this molecule in lymphocyte-endothelium cross talk remains unclear. In addition to its enzymatic role in the production of extracellular Ado, CD73 has also been characterized as a signaling molecule (31) and an adhesion molecule (32). Engagement of lymphocyte CD73 with anti-CD73 mAbs has been shown to stimulate proliferation, IL-2 secretion, and IL-2R expression (33, 34). Furthermore, blocking this molecule on lymphocytes with an Ab appears to inhibit adhesion of lymphocytes to cultured endothelial cells (35). Thus, there are multiple mechanisms by which CD73 could impact lymphocyte migration across HEV. We show in this study that *cd73*-deficient mice have increased rates of lymphocyte homing to draining lymph nodes, and propose that CD73-generated Ado regulates the ability of lymphocytes to migrate across HEV, thus limiting their access to inflamed lymph nodes.

Materials and Methods

Mice

Cd73-deficient mice developed in our laboratory ([illegible]) were backcrossed onto C57BL/6J for 14 generations. Genotyping by PCR using primers that differentiate between the wild-type *cd73* allele and the mutated *cd73* allele containing a neomycin resistance cassette was performed as previously described. $A_{2B}AR^{-/-}$ mice were obtained from Deltagen and have also been backcrossed onto the C57BL/6 background. All mice were bred and maintained in our animal facility under specific pathogen-free conditions. All protocols were approved by the Oklahoma Medical Research Foundation Institutional Animal Care and Use Committee.

Cell culture

The cell line KOP2.16 was derived from stromal cells taken from pooled mouse lymph nodes and has been described previously (36). It was cultured in DMEM supplemented with 20% FCS (HyClone), 10 mM HEPES, 1 mM sodium pyruvate, 2 mM L-glutamine, 5×10^{-5} M 2-ME, nonessential amino acids, 100 U/ml penicillin, and 100 μg/ml streptomycin. In some experiments, 20 ng/ml TNF-α (R&D Systems) was added for 3–6 h.

Cd73 and AR gene expression

Cd73 and AR expression were analyzed by PCR in a full-length cDNA library derived from MACS (Miltenyi Biotec)-isolated PNAd$^+$ endothelial cells from lymph nodes (37) using previously described primers (38). In other experiments, RNA was prepared from KOP2.16, and RT-PCR was performed as described using β-actin as an internal control (38).

Digestion of lymph nodes for characterization of HEV or enumeration of CD11c$^+$ dendritic cells (DC) by flow cytometry

Lymph nodes were dissected from mice, minced with scissors, and digested in RPMI 1640 containing 10% FCS, 1 mg/ml collagenase B (Roche), and 2 μg/ml DNase I (Roche) for 30 min at 37°C with shaking at 50 rpm. The cell suspension was passed through a Pasteur pipette 40 times, followed by digestion with 0.2% trypsin (Mediatech) and 0.5 mM EDTA at 37°C for 10 min. Cells were then passed through a 70-μm filter, washed, and stained.

Immunofluorescence

Lymphoid cells or PNAd$^+$ cells were stained with the following mAbs: FITC anti-CD4, FITC anti-CD8, FITC anti-MHC class II, PE anti-CD11c, PE-Cy5.5 anti-CD19, and allophycocyanin anti-CD45R (Caltag Laboratories); PE-anti-TCRβ (BD Pharmingen); allophycocyanin anti-CD45 (Southern Biotechnology Associates); and biotinylated anti-CD73 (TY/23) (39), according to standard methods. PE-streptavidin was from BD Pharmingen. Data were collected with a FACSCalibur (BD Biosciences) and analyzed with CellQuest software. For lymphocyte migration experiments and experiments to enumerate DC, data were collected on 750,000 and 350,000 cells, respectively.

Immunohistochemistry

Frozen sections (7 μm) of lymph nodes were fixed with cold acetone and blocked with 3% BSA in PBS. Sections were stained with TY/23 (anti-CD73, IgG2a), followed by Alexa Fluor 488-conjugated donkey anti-rat IgG (Molecular Probes), and then blocked with purified mouse IgG at 500 μg/ml. After washing, they were then stained with Alexa Fluor 594-conjugated anti-PNAd mAb MECA-79 (IgM; BD Pharmingen). Other slides were stained with a combination of TY/23 and rabbit anti-collagen IV (Chemicon International), followed by a combination of Alexa Fluor 488-conjugated donkey anti-rat IgG plus Alexa Fluor 594-conjugated donkey anti-rabbit IgG (Molecular Probes).

Inflammatory stimuli

Anesthetized mice were injected with 1 μg of *Escherichia coli* LPS (055:B5; Sigma-Aldrich) or 5 μg of poly(I:C) (Sigma-Aldrich) in 30 μl of PBS in the left front footpad using an insulin syringe. The right footpad was injected with same volume of PBS. Twenty-four hours later, brachial lymph nodes were examined as draining lymph nodes. In other experiments, mice were injected in either the rear footpad or thigh, and popliteal or inguinal lymph nodes, respectively, were studied as draining lymph nodes.

Lymphocyte homing assay

Total splenocytes were labeled with 0.25 μM 5-chloromethylfluorescein diacetate (CMFDA; Molecular Probes) for 30 min at 37°C. Ten million labeled cells were injected i.v. into mice, and 1 h later, spleen and lymph nodes were harvested. In some experiments, *cd73*-deficient and wild-type splenocytes were labeled with 0.25 μM CMFDA and 2 μM 5-(and-6)-(((4-chloromethyl)benzoyl)amino)tetramethylrhodamine (CMTMR; Molecular Probes), respectively, for 30 min at 37°C. Equal numbers of labeled cells were coinjected i.v. into both strains of mice. Harvested lymph nodes were pushed through 70-μm filters to make single-cell suspensions. Cells were then counted, and the percentages of labeled cells were determined by flow cytometry. In selected experiments, anti-L-selectin Ab (MEL-14; Southern Biotechnology Associates) was given to mice (50 μg/mouse) i.v. simultaneously with LPS. In other experiments, mice were pretreated with the $A_{2B}AR$ agonist BAY 60-6583 at 0.32 mg/kg (Bayer HealthCare) dissolved in polyethylene glycol (PEG) 400 and diluted to 80 μg/ml in PBS for i.v. injection 30 min before the injection of labeled splenocytes.

Results

CD73 and AR expression in lymphoid tissues and HEV

We previously reported the expression pattern of CD73 in lymphoid tissues of BALB/c mice (39); however, experiments indicating that CD73 expression was strain dependent prompted us to

investigate CD73 expression in lymphoid cells of C57BL/6 mice before using this strain for the experiments described in this study. Staining with mAb TY/23 revealed that ~50% of $CD4^+$, 85% of $CD8^+$, and 2% of $CD19^+$ lymphocytes derived from lymph nodes of wild-type mice expressed CD73 (Fig. 1*A*). We confirmed the findings of Kobie et al. (41) that CD73 is expressed on $CD4^+CD25^+Foxp3^+$ regulatory T cells. Nevertheless, $cd73^{+/+}$ and $cd73^{-/-}$ mice had similar proportions of T cells with this phenotype (data not shown). Lymphocytes from $cd73^{-/-}$ mice expressed no detectable CD73, confirming the deletion. We also analyzed CD73 expression on HEV by flow cytometry, gating on the rare population of CD45$^-$ $PNAd^+$ cells (0.05–0.15% of cells from enzyme-digested whole lymph nodes). Relatively high CD73 expression was observed on HEV compared with lymphocytes (Fig. 1*B*). To substantiate the results, immunohistochemistry was performed (Fig. 1*C*). Sections stained with anti-PNAd Ab and TY/23 revealed that HEV expressed CD73 abundantly. In contrast, only a few lymphocytes expressed enough CD73 to be detectable by this method. In addition, double staining with anti-collagen IV Ab and TY/23 demonstrated that CD73 is also expressed homogeneously on basal lamina (i.e., not polarized to the luminal or abluminal surface).

Steady-state mRNA levels of *cd73* and the AR were measured in HEV by PCR, using a cDNA library derived from $PNAd^+$ endothelial cells (Fig. 1*D*). *Cd73* and $A_{2B}AR$ were detected, but A_2AR, A_3AR, and A_1AR were not expressed at detectible levels. Steady-state levels of AR mRNA in murine splenocytes are shown in Fig. 1*E*. All AR except the A_1AR were easily detected.

CD73-deficient mice have large draining lymph nodes

CD73 has been proposed to modulate lymphocyte-endothelial cell interactions as an adhesion molecule (32, 35). Therefore, we asked whether CD73 plays a role in lymphocyte homing to secondary lymphoid tissue in the steady state. The sizes of spleen, peripheral lymph nodes, Peyer's patches, and mesenteric lymph nodes in *cd73*-deficient mice were normal (27 and our unpublished data). Furthermore, the migration of CMFDA-labeled $cd73^{-/-}$ splenocytes to lymphoid tissues (spleen and lymph node) of unmanipulated $cd73^{-/-}$ mice was also comparable to that of $cd73^{+/+}$ splenocytes to lymphoid organs of unmanipulated wild-type mice (our unpublished data). These observations suggested that CD73 does not have an obvious function in lymphocyte homing under steady-state conditions.

CD73 plays important roles in vivo in maintaining the integrity of the vascular endothelium during hypoxia (27–29) and in regulating endothelial adhesion molecule expression after wire-induced injury (30). Taking this information into account, and considering the well-known anti-inflammatory properties of Ado, we hypothesized that CD73 might also regulate lymphocyte-HEV interactions after an inflammatory stimulus. To address this issue, LPS was injected into front left footpads of $cd73^{+/+}$ and $cd73^{-/-}$ mice, and 24 h later, the brachial (draining) lymph node cellularity was examined (Fig. 2*A*). The same volume of PBS was administered to the contralateral side as a control. As expected from previous studies (14, 15), the draining lymph nodes were dramatically enlarged compared with those on the control side in wild-type mice. Consistent with our hypothesis, there was a further increase in the size of the draining lymph nodes from *cd73*-deficient mice, which were 1.5-fold larger than those of wild-type mice. To examine whether lymphocyte migration from the bloodstream to lymph nodes is also accelerated in $cd73^{-/-}$ mice, CMFDA-labeled wild-type splenocytes were injected i.v. 24 h after LPS injection and the accumulation of labeled cells in the lymph nodes was measured after 1 h by flow cytometry (Fig. 2*B*). Although no differences

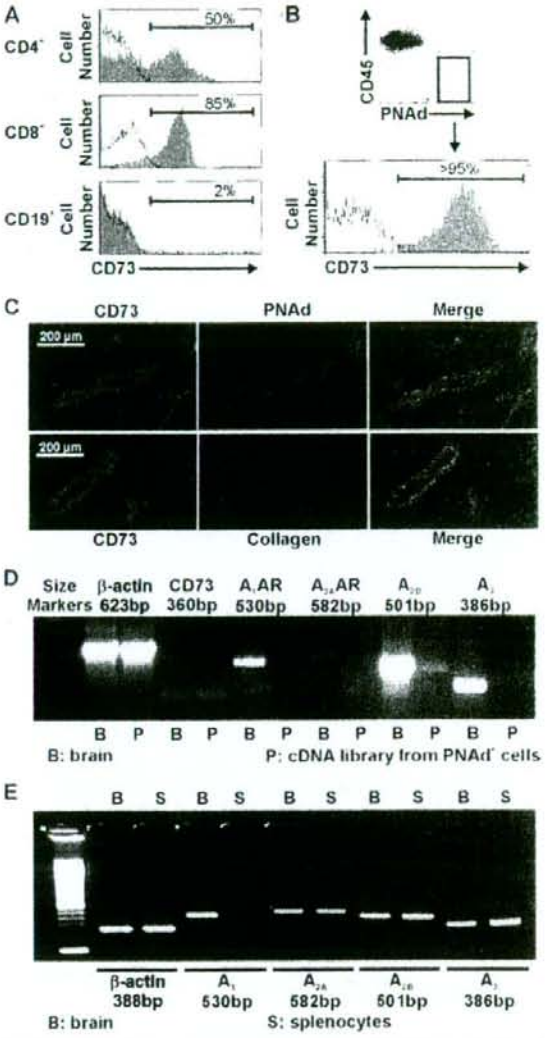

FIGURE 1. CD73 expression on lymphocytes and HEV. *A*, Single-cell suspensions of lymph node cells from $cd73^{+/+}$ and $cd73^{-/-}$ mice were stained with FITC anti-CD4, FITC anti-CD8, or PE-Cy5.5 anti-CD19 plus biotinylated anti-CD73 (TY/23) and PE-streptavidin or the relevant isotype-matched control Abs. CD73 expression in $cd73^{+/+}$ mice is shown in the shaded histograms, and that in $cd73^{-/-}$ mice is shown with solid lines. Staining with isotype control Abs is shown with dotted lines. The dotted lines and solid lines are virtually overlapping. *B*, Other lymph nodes from wild-type mice were digested with collagenase, DNase I, and trypsin, as described in *Materials and Methods*, and cells were stained with allophycocyanin anti-CD45, purified anti-PNAd plus Alexa Fluor 488 anti-IgM, and biotinylated anti-CD73 plus PE-streptavidin. HEV were identified as $CD45^-$ $PNAd^+$ cells. *C*, Frozen sections of lymph nodes were stained with anti-CD73 (TY/23) and either anti-PNAd or anti-collagen IV, as described in *Materials and Methods*. *D*, *Cd73* and AR expression were assessed by RT-PCR in a cDNA library derived from $PNAd^+$ endothelial cells. Representative results are shown from more than three experiments. *E*, AR expression was assessed by RT-PCR in total wild-type splenocytes. Representative results from more than three experiments are shown.

were observed between $cd73^{+/+}$ and $cd73^{-/-}$ mice on the control side, the number of lymphocytes that migrated into the draining lymph nodes of *cd73*-deficient mice was 2.7-fold greater than in

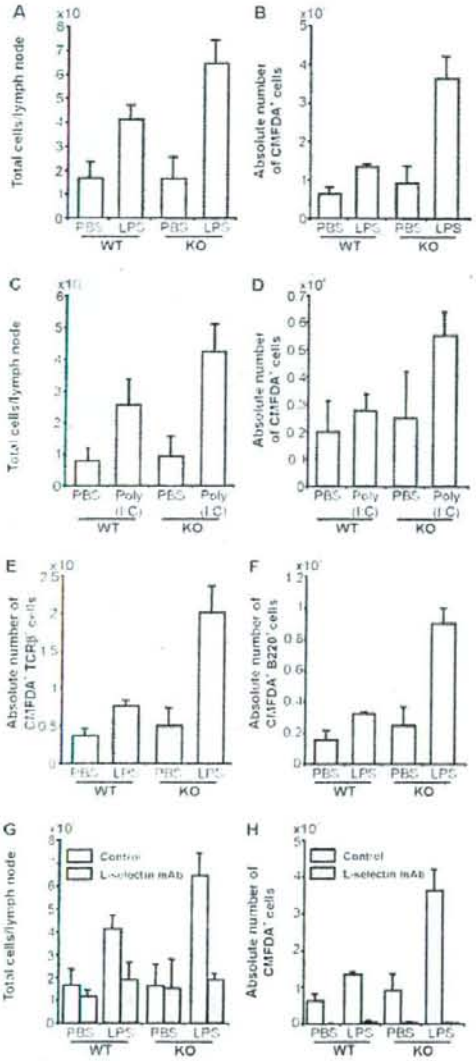

FIGURE 2. *Cd73*-deficient mice have large draining lymph nodes and high rates of L-selectin-dependent lymphocyte migration after an inflammatory stimulus. LPS (1 μg; *A*, *B*, *E*, *F*, *G*, and *H*) or poly(I:C) (5 μg; *C* and *D*) was injected into the left front footpad (or thigh; *C* and *D*) of $cd73^{+/+}$ and $cd73^{-/-}$ mice, and an equivalent volume of PBS was injected into the right front footpad (or thigh; *C* and *D*). Twenty-four hours later, the mice were injected with 10^7 CMFDA-labeled $cd73^{+/+}$ splenocytes i.v. One hour later, brachial (or inguinal; *C* and *D*) lymph nodes were harvested, and the total numbers of cells in each lymph node were counted. *A* and *C*, The lymph node cells were then stained with PE anti-TCRβ and allophycocyanin anti-B220 (CD45R). The percentages of fluorescent cells were determined by flow cytometry, and the absolute numbers of total lymphocytes (*B* and *D*), T cells (*E*), and B cells (*F*) that migrated to the lymph nodes in 1 h were calculated. In some experiments, the mice also received 50 μg of anti-L-selectin Ab MEL-14 i.v. at the same time as LPS/PBS. Twenty-four hours later, the mice were injected with 10^7 CMFDA-labeled $cd73^{+/+}$ splenocytes i.v. One hour later, lymph nodes were harvested and the total numbers of cells in each lymph node were counted (*G*). The percentages of CMFDA$^+$ cells were determined by flow cytometry, and the absolute numbers of total lymphocytes that migrated to the lymph nodes in 1 h were calculated (*H*). Data from mice not receiving anti-L-selectin Ab in *G* and *H* are the same as in *A* and *B*.

wild-type mice. These results suggest that it is CD73 on HEV (rather than on lymphocytes) that is responsible for the larger sizes of draining lymph nodes in *cd73*-deficient mice. Similar results were seen when poly(I:C), a TLR3 ligand, was used instead of LPS as the inflammatory stimulus (Fig. 2, *C* and *D*). Furthermore, staining with TCRβ (Fig. 2*E*) and B220 (Fig. 2*F*) Abs revealed that migration of both T and B lymphocytes was increased in *cd73*-deficient draining lymph nodes. Similar results were observed when LPS or poly(I:C) was injected into the rear footpad or thigh, as revealed by examination of popliteal or inguinal lymph nodes, respectively (our unpublished data).

Next, we asked whether the increased lymphocyte migration and enlarged lymph nodes seen in *cd73*-deficient mice were the result of increased migration across HEV. To address this question, mice were pretreated with L-selectin Ab. This Ab was chosen because lymphocyte-expressed L-selectin is known to initiate rolling on HEV (through its interaction with PNAd) and because administration of L-selectin Ab has been shown to diminish lymphocyte migration to peripheral lymph nodes under steady-state conditions in vivo (3, 42). We observed that treatment of mice with L-selectin Ab i.v. at the same time as LPS abrogated CMFDA-labeled lymphocyte migration even after 24 h in both strains of mice (Fig. 2*H*) and abolished the hallmark increased size of *cd73*-deficient draining lymph nodes (Fig. 2*G*).

Contribution of lymphocyte CD73 expression to migration across HEV

Because lymphocyte CD73 has been reported to be a signaling molecule, an adhesion molecule, and a maturation and subpopulation marker (16, 39), we next evaluated its role in lymphocyte migration into draining lymph nodes. We first examined the percentage of CD4$^+$, CD8$^+$, and CD19$^+$ lymphocytes that co-expressed CD73 in wild-type draining lymph nodes by flow cytometry 24 h after stimulation. LPS-induced lymph node hypertrophy did not affect the CD73 expression pattern compared with that in lymph nodes from the PBS-treated side (Fig. 3*A*). The CD73 expression pattern was also equivalent to that in naive lymph nodes and spleen (our unpublished data). We next evaluated migration of *cd73*-deficient lymphocytes compared with wild-type lymphocytes in both wild-type and *cd73*-deficient mice. This was done by injecting mice with a 1:1 mixture of splenocytes from $cd73^{+/+}$ and $cd73^{-/-}$ mice labeled with either CMFDA or CMTMR. Virtually identical ratios of $cd73^{-/-}$:$cd73^{+/+}$ lymphocytes were observed in both wild-type and *cd73*-deficient draining lymph nodes (Fig. 3*B*). These results suggest no bias between CD73-positive and -negative lymphocytes in their ability to migrate after an inflammatory stimulus. They further suggest that it is a lack of CD73 expression on HEV that is responsible for the increased migration of lymphocytes into draining lymph nodes of *cd73*-deficient mice.

Contribution of DC to increased draining lymph node size in $cd73^{-/-}$ *mice*

The accumulation of activated DC in draining lymph nodes is critical for the regulation of proinflammatory cytokine production and induction of vascular growth (15). Local injection of LPS is known

All results are expressed as mean ± SD and are representative of 3–10 experiments ($n = 4$–5 mice of each genotype for each experiment, $p \leq 0.025$ for all comparisons of wild type (WT) vs knockout (KO) in draining lymph nodes in *A*–*F*, for control vs MEL-14 in draining lymph nodes for *G*, and for control vs MEL-14 in all groups in *H*).

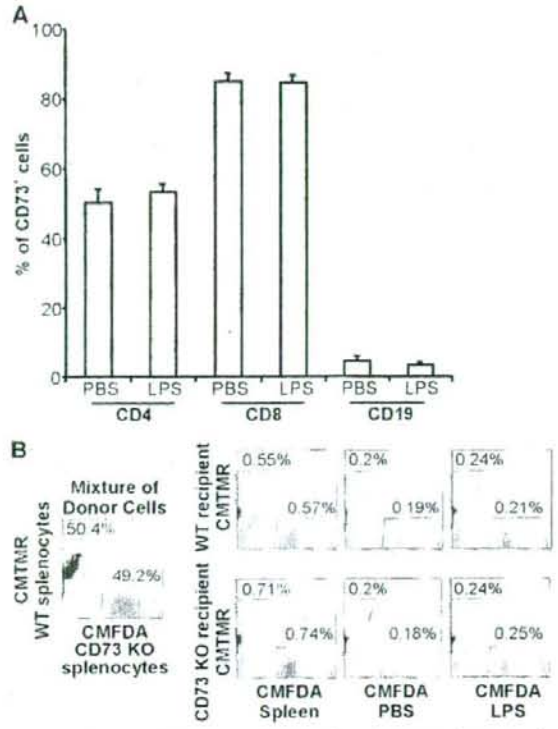

FIGURE 3. CD73-positive and -negative lymphocytes migrate equally well into inflamed lymph nodes. LPS (1 μg) was injected into the left rear footpad of *cd73*$^{+/+}$ mice, and an equivalent volume of PBS was injected into the right rear footpad. *A*, Twenty-four hours later, the popliteal lymph node cells were stained with FITC anti-CD4, FITC anti-CD8, or PE Cy5.5 anti-CD19 plus biotinylated anti-CD73 (TY/23) and PE-streptavidin or the relevant isotype-matched control Abs, and the percentages of CD4$^+$, CD8$^+$, and CD19$^+$ lymphocytes that coexpressed CD73 were determined by flow cytometry ($n = 4$ in each of two independent experiments). *B*, LPS (1 μg) was injected into the left thigh of *cd73*$^{-/-}$ and *cd73*$^{+/+}$ mice, and an equivalent volume of PBS was injected into the right thigh. Twenty four hours later, the mice were injected i.v. with an equal mixture of 1×10^7 *cd73*$^{+/+}$ and *cd73*$^{-/-}$ splenocytes labeled with CMFDA or CMTMR, respectively. One hour later, inguinal lymph nodes were harvested, and the percentages of CMFDA$^+$ and CMTMR$^+$ lymphocytes were determined. Representative data from one of two experiments are shown.

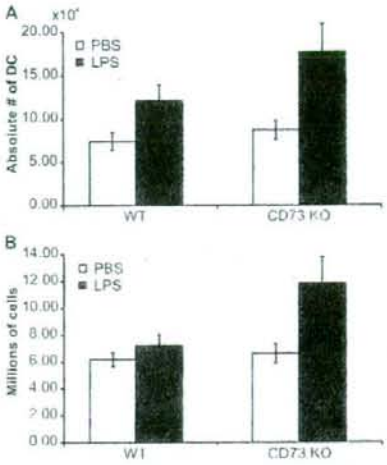

FIGURE 4. Migration of DC into draining lymph nodes after an inflammatory stimulus. LPS (1 μg) was injected into the left front footpad of *cd73*$^{+/+}$ and *cd73*$^{-/-}$ mice, and an equivalent volume of PBS was injected into the right front footpad. Six hours later, lymph nodes were digested with collagenase, DNase I, and trypsin, as described in *Materials and Methods*, and cells were counted and stained with FITC anti-MHC class II and PE anti-CD11c. Dead cells were excluded by propidium iodide staining. The average (±SEM) absolute numbers of MHC class II^{high} CD11c$^+$ cells are shown (*A*) as well as the total number of leukocytes/lymph node (*B*). The results are combined from two experiments with a total of nine mice/group. Value of $p = 0.14$ for the number of MHC class II^{high} CD11c$^+$ cells in draining lymph nodes of wild-type vs *cd73*$^{-/-}$ mice, and $p = 0.034$ for the comparison of total cell numbers/lymph node.

to induce DC migration to draining lymph nodes through the lymphatics and also their maturation and cytokine production (13). Because previous reports showed that Ado is one of the key regulators of DC function (43, 44), we speculated that the hypertrophied draining lymph nodes in *cd73*$^{-/-}$ mice might be due to increased migration of DC though the lymphatics. Therefore, we measured the absolute numbers of MHC class II^{high} CD11c$^+$ DC in the draining lymph nodes of wild-type and *cd73*$^{-/-}$ mice 6 h after the injection of LPS (Fig. 4*A*). As expected, the numbers of DC were increased in the draining lymph nodes of both strains of mice compared with those on the contralateral side. There was a trend toward higher numbers of DC in the draining lymph nodes of *cd73*$^{-/-}$ mice, because the average number was almost 50% higher than for wild-type mice; however, this difference was not statistically significant ($p = 0.14$). Nevertheless, these data suggest that increased cytokine production by DC could contribute to the larger size of draining lymph nodes in *cd73*$^{-/-}$ mice. It is interesting to note that the draining lymph nodes in the *cd73*$^{-/-}$ mice were significantly larger than those of wild-type mice ($p = 0.034$) even at this early time point (Fig. 4*B*), suggesting that the kinetics of the inflammatory response are accelerated when CD73 is absent.

Up-regulation of CD73 and $A_{2B}AR$ on HEV after an inflammatory stimulus

Previous studies showed CD73 expression can be regulated on HUVEC by mediators that are released during an inflammatory response, such as TNF-α (45), IFN-α (46), and Ado (47). Flow cytometry revealed a slight up-regulation of cell surface CD73 on CD45$^-$ PNAd$^+$ cells in draining lymph nodes relative to its level on HEV from control lymph nodes (Fig. 5*A*). Due to the lack of specific AR Abs suitable for flow cytometry, we used KOP2.16, a cell line derived from lymph node endothelial cells, and semiquantitative RT-PCR to examine the regulation of AR expression. Similar to what we observed in the HEV cDNA library (Fig. 1*D*), KOP2.16 expressed only the $A_{2B}AR$. Expression increased 3- to 5-fold 3 h after TNF-α stimulation in two independent experiments (Fig. 5*B*). These results suggest that elevated Ado, known to occur at sites of inflammation, could trigger the A_{2B}AR on HEV in draining lymph nodes, and that this could play a role in regulating lymphocyte migration into these nodes.

AR stimulation inhibits the increased lymphocyte migration into draining lymph nodes of CD73-deficient mice

Our previous findings and those of others suggest that Ado generated extracellularly by CD73 can modulate endothelial cell

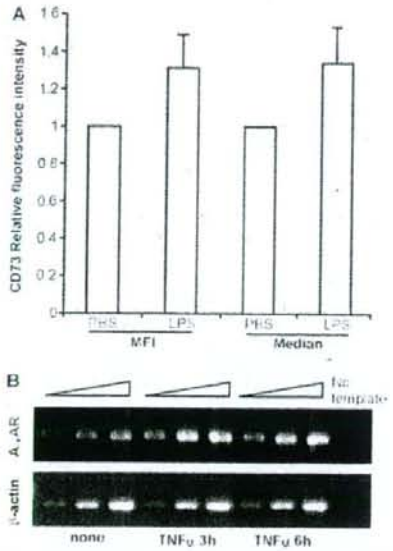

FIGURE 5. CD73 and the $A_{2B}AR$ are up-regulated on HEV after an inflammatory stimulus. *A*, LPS (1 μg) was injected into the left front footpad of *cd73*$^{+/+}$ mice, and an equivalent volume of PBS was injected into the right front footpad. Twenty-four hours later, lymph nodes were digested with collagenase, DNase I, and trypsin, as described in *Materials and Methods*, and cells were stained with allophycocyanin anti-CD45, purified anti-PNAd plus Alexa Fluor 488 anti-IgM, and biotinylated anti-CD73 plus PE-streptavidin. HEV were identified as CD45$^-$ PNAd$^+$ cells. The relative mean (MFI) and median fluorescence intensities for CD73 staining are shown (mean ± SD, total $n = 8$ from three independent experiments, $p < 0.01$ for MFI, and $p < 0.02$ for median fluorescence intensities in paired t tests comparing PNAd$^+$ cells from inflamed and control lymph nodes). *B*, KOP2.16 cells were cultured ± TNF-α for 3–6 h. RNA was isolated and $A_{2B}AR$ expression was determined by semiquantitative RT-PCR on 5-fold serial dilutions of cDNA using β-actin expression as an internal standard. Data are representative of one of two experiments. Quantitation of the band intensities revealed a 5-fold increase in $A_{2B}AR$ mRNA at 3 h and a 2.5-fold increase at 6 h relative to β-actin expression.

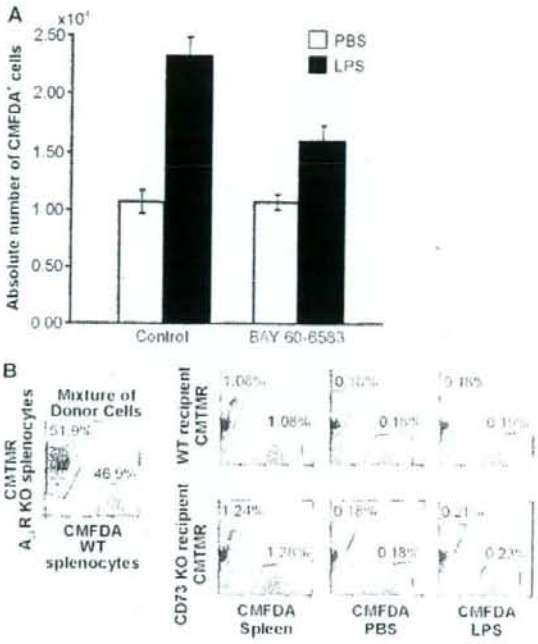

FIGURE 6. The A_{2B} AR agonist, BAY 60-6583, inhibits the increased lymphocyte migration into draining lymph nodes of CD73-deficient mice. *A*, LPS (1 μg) was injected into the left front footpad of *cd73*$^{+/+}$ and *cd73*$^{-/-}$ mice, and an equivalent volume of PBS was injected into the right front footpad. Twenty-two hours and 30 min after the LPS injection, the mice were injected i.v. with BAY 60-6583 (320 μg/kg) or an equivalent volume of diluted PEG 400 carrier, and 30 min later with 10^7 CMFDA-labeled *cd73*$^{+/+}$ splenocytes. One hour after the injection of labeled splenocytes, lymph nodes were harvested, the total numbers of cells in each lymph node were counted, and the percentages of CMFDA$^+$ cells were determined by flow cytometry ($n = 20–26$; $p = 0.0034$ for diluted PEG 400 vs BAY 60-6583 in draining lymph nodes; data combined from four separate experiments). *B*, LPS (1 μg) was injected into the left front footpad of wild-type and *cd73*$^{-/-}$ mice, and an equivalent volume of PBS was injected into the right front footpad (five mice/group). Twenty-three hours later, the mice were injected i.v. with an equal mixture of 10^7 wild-type and $A_{2B}R^{-/-}$ splenocytes labeled with CMFDA or CMTMR, respectively. One hour later, brachial lymph nodes were harvested, and the percentages of CMFDA$^+$ and CMTMR$^+$ lymphocytes were determined by flow cytometry. Data are representative of one of two experiments.

adhesion molecule expression and permeability via the A_{2A}AR and A_{2B}AR (27–30). Based on these findings, and our own observation that the A_{2B}R was the only AR expressed on HEV, we asked whether the A_{2B}AR-specific agonist BAY 60-6583 could influence lymphocyte homing after an inflammatory stimulus. As shown in Fig. 6*A*, treatment with BAY 60-6583 markedly decreased ($p = 0.0034$) the number of lymphocytes that migrated into the draining lymph nodes of CD73-deficient mice. There was no impact on lymphocyte migration into lymph nodes on the contralateral side. The effect of BAY 60-6583 on lymphocyte migration into draining lymph nodes of wild-type mice was much more modest and did not reach statistical significance (data not shown), perhaps because of higher concentrations of endogenous Ado in these mice. All of these results support our hypothesis that CD73 generated Ado serves to regulate lymphocyte migration into draining lymph nodes after an inflammatory stimulus at least in part by triggering A_{2B}AR signaling on HEV. Consistent with this hypothesis, $A_{2B}AR^{-/-}$ and $A_{2B}AR^{-/-}$ lymphocytes showed equivalent rates of lymphocyte migration into draining lymph nodes of LPS-treated wild-type and *cd73*$^{-/-}$ mice (Fig. 6*B*).

Discussion

Lymphocyte homing to peripheral lymph nodes depends on interactions with HEV, specialized blood vessels that express chemokines, and adhesion molecules required for lymphocyte transmigration. Although numerous reports have demonstrated the importance of L-selectin, PNAd, LFA-1, ICAM-1, and specific chemokines and chemokine receptors in the steady state, the way in which lymphocyte migration across HEV is regulated during an inflammatory response is not fully understood. The goal of this investigation was to determine whether CD73, which is expressed on both PNAd$^+$ endothelial cells and the basal lamina comprising HEV, plays a role in this process. The source of CD73 expressed on basal lamina is not known. However, CD73 is a GPI-anchored protein, and previous studies by Mehul et al. (18) showed that CD73 can bind to laminin, one of the components of the basal lamina. Therefore, we hypothesize that CD73 may be synthesized in cells such as endothelial cells, cleaved from the cell surface by

a phospholipase, and then bind to a component of the basal lamina such as laminin.

The contribution of CD73 to the formation of extracellular Ado, a well-known anti-inflammatory mediator, has been revealed in several experimental models. For example, the anti-inflammatory action of methotrexate in the carrageenan-treated air pouch model of inflammation is dependent upon CD73 (49). Similarly, CD73-generated Ado is necessary for ischemic preconditioning in both the heart (40) and kidney (50), and protects mice from bleomycin-induced lung injury (51). Furthermore, *cd73*-deficient mice exhibit a vascular leak syndrome characterized by neutrophil infiltration into tissues when exposed to normobaric hypoxia, suggesting a critical role for CD73-generated Ado in vascular barrier function (27–29). In contrast, several in vitro studies suggested that CD73 functions as a costimulatory molecule on T lymphocytes (33, 34) and an adhesion molecule that is important for lymphocyte binding to endothelium (35). The possibility that CD73 could impact lymphocyte interactions with HEV by multiple mechanisms prompted us to examine the role of this molecule in lymphocyte homing to lymph nodes. We showed in this study that Ado generated by CD73 on HEV negatively regulates lymphocyte migration from the bloodstream into LPS-induced draining lymph nodes. Because $cd73^{+/-}$ and $cd73^{-/-}$ splenocytes showed equivalent rates of migration into draining lymph nodes, it is unlikely that any signaling or adhesive function of CD73 on lymphocytes plays a role in regulating migration of lymphocytes across HEV.

Although no abnormalities were observed in the cellularity of lymphoid organs of $cd73^{-/-}$ mice or in the migratory capacity of $cd73^{-/-}$ lymphocytes under steady-state conditions, $cd73^{-/-}$ mice had larger draining lymph nodes when LPS, a TLR4 agonist, was injected into a local site. Short-term assays with CMFDA-labeled lymphocytes administered i.v. showed increased rates of migration into the draining lymph nodes of $cd73^{-/-}$ mice. This observation, coupled with the forward vs side scatter profile of the lymphocytes (our unpublished data), suggested that the lymph node hypertrophy induced by LPS was not due to the proliferation of lymphocytes, but rather to the accumulation of nondividing lymphocytes. Furthermore, anti-L-selectin Ab treatment demonstrated that CD73 modulates lymphocyte migration into draining lymph nodes by an L-selectin-dependent pathway. Interestingly, both T and B lymphocyte entrance was promoted in $cd73^{-/-}$ mice, suggesting that a common pathway for both cell types is modulated by CD73. In addition, the percentages of $CD73^+$ and $CD73^-$ lymphocytes did not change when splenocytes from $cd73^{+/+}$ mice were used as donors in migration experiments in $cd73^{+/+}$ mice, indicating that the ability to migrate across HEV was not influenced by the CD73 expression status of lymphocytes. Furthermore, the migration of splenocytes from $cd73^{+/+}$ and $cd73^{-/-}$ mice into draining lymph nodes of $cd73^{-/-}$ mice was comparable, demonstrating that CD73 expression on lymphocytes cannot compensate for a lack of CD73 on HEV.

Information in the literature concerning the regulation of endothelial CD73 expression by proinflammatory cytokines is conflicting. For example, Kalsi et al. (45) showed a decrease in its expression and in its enzyme activity after TNF-α treatment of HUVEC. In contrast, Niemela et al. (46) demonstrated that IFN-α and IFN-γ, but not other inflammatory cytokines such as IL-1β, IL-4, or TNF-α, could increase CD73 expression on HUVEC. Furthermore, Ado has been implicated in an increase in CD73 expression in microvascular endothelial cells that is mediated by a paracrine pathway (47). Our experiments revealed that the expression of CD73 on HEV in draining lymph nodes is up-regulated compared with HEV in the contralateral side. Although our analysis has the advantage of evaluating changes in CD73 expression in vivo, the mechanism by which CD73 expression is modulated is still unknown.

To determine whether the enhanced lymphocyte migration in *cd73*-deficient mice was caused by a lack of AR signaling, we treated mice with the $A_{2B}R$ agonist BAY 60-6583. This approach was taken because of the four known subtypes of AR; only the $A_{2B}AR$ was found in a cDNA library derived from $PNAd^+$ cells or in cDNA from the HEV-like cell line KOP2.16 (36). We also observed an up-regulation of $A_{2B}AR$ expression in KOP2.16 cells after exposure to TNF-α. Indeed, BAY 60-6583 treatment markedly reduced the rate of migration of labeled splenocytes into draining lymph nodes of $cd73^{-/-}$ mice. These data are consistent with the hypothesis that the $A_{2B}AR$ is at least partially responsible for the regulation of lymphocyte migration across HEV by CD73-generated Ado. Furthermore, the Ado is most likely derived from CD73 on HEV, because lymphocytes from $cd73^{+/+}$ and $cd73^{-/-}$ mice show similar increased rates of migration across HEV in draining lymph nodes of $cd73^{-/-}$ mice (i.e., Ado produced by $cd73^{+}$ lymphocytes does not appear able to trigger AR on HEV to regulate lymphocyte migration). Similarly, lymphocytes from $A_{2B}R^{+/+}$ and $A_{2B}R^{-/-}$ mice showed similar rates of migration into draining lymph nodes of wild-type mice, suggesting that it is triggering of the $A_{2B}R$ on HEV that is relevant.

The expression of the adhesion molecules ICAM-1 and VCAM-1 is normal on $cd73^{-/-}$ HEV in the steady state (our unpublished data). Our findings differ from those in a previous report (30), which concluded that CD73 deficiency resulted in increased VCAM-1 expression and decreased ICAM-1 expression on carotid arteries due to the lack of $A_{2A}AR$ signaling. This discrepancy could be explained by the fact that different cell types were being examined and that the $A_{2B}AR$, rather than the $A_{2A}AR$, seems to be the predominant AR on HEV. We did find that VCAM-1, but not ICAM-1, expression was up-regulated on HEV in draining lymph nodes after LPS administration and this effect was more pronounced in $cd73^{-/-}$ mice. However, neither anti-VLA-4 nor anti-VCAM-1 Ab treatment reversed the increased rates of lymphocyte migration into draining lymph nodes of $cd73^{-/-}$ mice after LPS treatment (our unpublished data), suggesting that the increase in VCAM-1 expression did not augment cell adhesion between lymphocytes and HEV. Furthermore, although the migration of CMFDA-labeled lymphocytes to draining lymph nodes was inhibited by treatment with an anti-LFA-1 Ab, the effect was the same in both $cd73^{+/+}$ and $cd73^{-/-}$ mice (our unpublished data). Taken together, these data support the conclusion that increased lymphocyte migration into draining lymph nodes of *cd73*-deficient mice is not mediated by increases in cell adhesion.

We propose instead that Ado generated by endothelial cell (and/or basal lamina) CD73 regulates lymphocyte migration across HEV through $A_{2B}AR$ signaling. The $A_{2B}AR$ is a seven-transmembrane-spanning G protein-coupled receptor that is coupled to G_s and uses cAMP as a second messenger (52). It has been firmly established that cAMP can modulate endothelial cell-cell junctions through the protein kinase A and/or Epac-Rap1 pathways (53, 54). Other reports suggest that the $A_{2B}AR$ can also be coupled to G_q (55). In the 1970s, several studies concluded that lymph node vasculature changed within 24 h after an inflammatory stimulus, and that this was associated with changes in vascular integrity (56, 57). Our studies do not address the mechanisms by which rates of lymphocyte migration are increased after an inflammatory stimulus, but do suggest that CD73-generated Ado may trigger a feedback mechanism to keep increases in permeability under control. Additional experiments with endothelial cell lines will be required to determine whether AR signaling modulates the ability of lymphocytes to migrate across HEV through changes in myosin L chain

phosphorylation and decreased formation of stress fibers and/or through Rap1/Epac-mediated increases in VE-cadherin-based cell-cell contacts. Future work will also address the consequences of increased lymphocyte migration into $cd73^{-/-}$ draining lymph nodes during an immune response.

Acknowledgments

We acknowledge Mary Flynn for manuscript preparation, the excellent technical assistance of Scott Hooker and Patrick Marble, and the expertise of Julie Maier in the Oklahoma Medical Research Foundation Imaging Facility. We also thank Dr. Paul Kincade for critical comments during manuscript preparation, Dr. Rob Welner for assistance with i.v. injections, and Drs. Almut Grenz and Tobias Eckle for advice regarding the administration of BAY 60-6583.

Disclosures

Thomas Krahn is an employee of Bayer HealthCare, the manufacturer of BAY 60-6583. All other authors have no conflicting financial interests.

References

1. Kraal, G., and R. E. Mebius. 1997. High endothelial venules: lymphocyte traffic control and controlled traffic. *Adv. Immunol.* 65: 347–395.
2. Miyasaka, M., and T. Tanaka. 2004. Lymphocyte trafficking across high endothelial venules: dogmas and enigmas. *Nat. Rev. Immunol.* 4: 360–370.
3. Rosen, S. D. 2004. Ligands for L-selectin: homing, inflammation, and beyond. *Annu. Rev. Immunol.* 22: 129–156.
4. Hamann, A., D. Jablonski-Westrich, A. Duijvestijn, E. C. Butcher, H. Baisch, R. Harder, and H. G. Thiele. 1988. Evidence for an accessory role of LFA-1 in lymphocyte-high endothelium interaction during homing. *J. Immunol.* 140: 693–699.
5. Campbell, J. J., J. Hedrick, A. Zlotnik, M. A. Siani, D. A. Thompson, and E. C. Butcher. 1998. Chemokines and the arrest of lymphocytes rolling under flow conditions. *Science* 279: 381–384.
6. Arbones, M. L., D. C. Ord, K. Ley, H. Ratech, C. Maynard-Curry, G. Otten, D. J. Capon, and T. F. Tedder. 1994. Lymphocyte homing and leukocyte rolling and migration are impaired in L-selectin-deficient mice. *Immunity* 1: 247–260.
7. Berlin-Rufenach, C., F. Otto, M. Mathies, J. Westermann, M. J. Owen, and A. Hamann. 1999. Lymphocyte migration in lymphocyte function-associated antigen (LFA)-1-deficient mice. *J. Exp. Med.* 189: 1467–1478.
8. Uchimura, K., J.-M. Gauguet, M. S. Singer, D. Tsay, R. Kannagi, T. Muramatsu, U. H. von Andrian, and S. D. Rosen. 2005. A major class of L-selectin ligands is eliminated in mice deficient in two sulfotransferases expressed in high endothelial venules. *Nat. Immunol.* 6: 1105–1113.
9. Butcher, E. C., M. Williams, K. Youngman, L. Rott, and M. Briskin. 1999. Lymphocyte trafficking and regional immunity. *Adv. Immunol.* 72: 209–253.
10. Mitoma, J., X. Bao, B. Petryniak, P. Schaerli, J. M. Gauguet, S. Y. Yu, H. Kawashima, H. Saito, K. Ohtsubo, J. D. Marth, et al. 2007. Critical functions of N-glycans in L-selectin-mediated lymphocyte homing and recruitment. *Nat. Immunol.* 8: 409–418.
11. Takeda, K., T. Kaisho, and S. Akira. 2003. Toll-like receptors. *Annu. Rev. Immunol.* 21: 335–376.
12. Roake, J. A., A. S. Rao, P. J. Morris, C. P. Larsen, D. F. Hankins, and J. M. Austyn. 1995. Dendritic cell loss from nonlymphoid tissues after systemic administration of lipopolysaccharide, tumor necrosis factor, and interleukin 1. *J. Exp. Med.* 181: 2237–2247.
13. Tsujimoto, H., T. Uchida, P. A. Efron, P. O. Scumpia, A. Verma, T. Matsumoto, S. K. Tschoeke, R. F. Ungaro, S. Ono, S. Seki, et al. 2005. Flagellin enhances NK cell proliferation and activation directly and through dendritic cell-NK cell interactions. *J. Leukocyte Biol.* 78: 888–897.
14. Soderberg, K. A., G. W. Payne, A. Sato, R. Medzhitov, S. S. Segal, and A. Iwasaki. 2005. Innate control of adaptive immunity via remodeling of lymph node feed arteriole. *Proc. Natl. Acad. Sci. USA* 102: 16315–16320.
15. Webster, B., E. H. Ekland, L. M. Agle, S. Chyou, R. Ruggieri, and T. T. Lu. 2006. Regulation of lymph node vascular growth by dendritic cells. *J. Exp. Med.* 203: 1903–1913.
16. Thompson, L. F., J. M. Ruedi, A. Glass, G. Moldenhauer, P. Moller, M. G. Low, M. R. Klemens, M. Massaia, and A. H. Lucas. 1990. Production and characterization of monoclonal antibodies to the glycosyl phosphatidylinositol-anchored lymphocyte differentiation antigen ecto-5′-nucleotidase (CD73). *Tissue Antigens* 35: 9–19.
17. Linden, J. 2001. Molecular approach to adenosine receptors: receptor-mediated mechanisms of tissue protection. *Annu. Rev. Pharmacol. Toxicol.* 41: 775–787.
18. Franco, R., A. Valenzuela, C. Lluis, and J. Blanco. 1998. Enzymatic and extraenzymatic role of ecto-adenosine deaminase in lymphocytes. *Immunol. Rev.* 161: 27–42.
19. Dong, R. P., J. Kameoka, M. Hegen, T. Tanaka, Y. H. Xu, S. F. Schlossman, and C. Morimoto. 1996. Characterization of adenosine deaminase binding to human CD26 on T cells and its biologic role in immune response. *J. Immunol.* 156: 1349–1355.
20. Hashikawa, T., S. W. Hooker, J. G. Maj, C. J. Knott-Craig, M. Takedachi, S. Murakami, and L. F. Thompson. 2004. Regulation of adenosine receptor engagement by ecto-adenosine deaminase. *FASEB J.* 18: 131–133.
21. Sun, D., L. C. Samuelson, T. Yang, Y. Huang, A. Paliege, T. Saunders, J. Briggs, and J. Schnermann. 2001. Mediation of tubuloglomerular feedback by adenosine: evidence from mice lacking adenosine 1 receptors. *Proc. Natl. Acad. Sci. USA* 98: 9983–9988.
22. Ledent, C., J.-M. Vaugeois, S. N. Schiffmann, T. Pedrazzini, M. El Yacoubi, J.-J. Vanderhaeghen, J. Costentin, J. K. Heath, G. Vassart, and M. Parmentier. 1997. Aggressiveness, hypoalgesia and high blood pressure in mice lacking the adenosine A_{2a} receptor. *Nature* 388: 674–678.
23. Chen, J. F., Z. Huang, J. Ma, J. Zhu, R. Moratalla, D. Standaert, M. A. Moskowitz, J. S. Fink, and M. A. Schwarzschild. 1999. A_{2A} adenosine receptor deficiency attenuates brain injury induced by transient focal ischemia in mice. *J. Neurosci.* 19: 9192–9200.
24. Yang, D., Y. Zhang, H. G. Nguyen, M. Koupenova, A. K. Chauhan, M. Makitalo, M. R. Jones, C. St. Hilaire, D. C. Seldin, P. Toselli, et al. 2006. The A2B adenosine receptor protects against inflammation and excessive vascular adhesion. *J. Clin. Invest.* 116: 1913–1923.
25. Salvatore, C. A., S. L. Tilley, A. M. Latour, D. S. Fletcher, B. H. Koller, and M. A. Jacobson. 2000. Disruption of the A_3 adenosine receptor gene in mice and its effect on stimulated inflammatory cells. *J. Biol. Chem.* 275: 4429–4434.
26. Cronstein, B. N. 1994. Adenosine, an endogenous anti-inflammatory agent. *J. Appl. Physiol.* 76: 5–13.
27. Thompson, L. F., H. K. Eltzschig, J. C. Ibla, C. J. Van De Wiele, R. Resta, J. C. Morote-Garcia, and S. P. Colgan. 2004. Crucial role for ecto-5′-nucleotidase (CD73) in vascular leakage during hypoxia. *J. Exp. Med.* 200: 1395–1405.
28. Eltzschig, H. K., L. F. Thompson, J. Karhausen, R. J. Cotta, J. C. Ibla, S. C. Robson, and S. P. Colgan. 2004. Endogenous adenosine produced during hypoxia attenuates neutrophil accumulation: coordination by extracellular nucleotide metabolism. *Blood* 104: 3986–3992.
29. Eckle, T., M. Faigle, A. Grenz, S. Laucher, L. F. Thompson, and H. K. Eltzschig. 2008. A2B adenosine receptor dampens hypoxia-induced vascular leak. *Blood* 111: 2024–2035.
30. Zernecke, A., K. Bidzhekov, B. Ozuyaman, L. Fraemohs, E. A. Liehn, J. M. Luscher-Firzlaff, B. Luscher, J. Schrader, and C. Weber. 2006. CD73/ecto-5′-nucleotidase protects against vascular inflammation and neointima formation. *Circulation* 113: 2120–2127.
31. Resta, R., Y. Yamashita, and L. F. Thompson. 1998. Ecto-enzyme and signaling functions of lymphocyte CD73. *Immunol. Rev.* 161: 95–109.
32. Airas, L., J. Niemela, and S. Jalkanen. 2000. CD73 engagement promotes lymphocyte binding to endothelial cells via a lymphocyte function-associated antigen-1-dependent mechanism. *J. Immunol.* 165: 5411–5417.
33. Massaia, M., L. Perrin, A. Bianchi, J. Ruedi, C. Attisano, D. Altieri, G. T. Rijkers, and L. F. Thompson. 1990. Human T cell activation. Synergy between CD73 (ecto-5′-nucleotidase) and signals delivered through CD3 and CD2 molecules. *J. Immunol.* 145: 1664–1674.
34. Dianzani, U., V. Redoglia, M. Bragardo, C. Attisano, A. Bianchi, D. DiFranco, U. Ramenghi, H. Wolff, L. F. Thompson, A. Pileri, and M. Massaia. 1993. Co-stimulatory signal delivered by CD73 molecule to human $CD45RA^{hi}CD45RO^{lo}$ (naive) $CD8^+$ T lymphocytes. *J. Immunol.* 151: 3961–3970.
35. Airas, L., J. Hellman, M. Salmi, P. Bono, T. Puurunen, D. J. Smith, and S. Jalkanen. 1995. CD73 is involved in lymphocyte binding to the endothelium: characterization of lymphocyte vascular adhesion protein 2 identifies it as CD73. *J. Exp. Med.* 182: 1603–1608.
36. Toyama-Sorimachi, N., K. Miyake, and M. Miyasaka. 1993. Activation of CD44 induces ICAM-1/LFA-1-independent, Ca^{2+}, Mg^{2+}-independent adhesion pathway in lymphocyte-endothelial cell interaction. *Eur. J. Immunol.* 23: 439–446.
37. Umemoto, E., T. Tanaka, H. Kanda, S. Jin, K. Tohya, K. Otani, K. Matsutani, M. Matsumoto, Y. Ebisuno, M. H. Jang, et al. 2006. Nepmucin, a novel HEV sialomucin, mediates L-selectin-dependent lymphocyte rolling and promotes lymphocyte adhesion under flow. *J. Exp. Med.* 203: 1603–1614.
38. Van De Wiele, C. J., J. G. Vaughn, M. R. Blackburn, C. Ledent, M. Jacobson, H. Jiang, and L. F. Thompson. 2002. Adenosine kinase inhibition promotes survival of fetal adenosine deaminase-deficient thymocytes by blocking dATP accumulation. *J. Clin. Invest.* 110: 395–402.
39. Yamashita, Y., S. W. Hooker, H. Jiang, A. B. Laurent, R. Resta, K. Khare, A. Coe, P. W. Kincade, and L. F. Thompson. 1998. CD73 expression and fyn-dependent signaling on murine lymphocytes. *Eur. J. Immunol.* 28: 2981–2990.
40. Eckle, T., T. Krahn, A. Grenz, D. Köhler, M. Mittelbronn, C. Ledent, M. Jacobson, H. Osswald, L. F. Thompson, K. Unertl, and H. K. Eltzschig. 2007. Cardioprotection by ecto-5′-nucleotidase (CD73) and A2B adenosine receptors. *Circulation* 115: 1581–1590.
41. Kobie, J. J., P. R. Shah, L. Yang, J. A. Rebhahn, D. J. Fowell, and T. R. Mosmann. 2006. T regulatory and primed uncommitted CD4 T cells express CD73, which suppresses effector CD4 T cells by converting 5′-adenosine monophosphate to adenosine. *J. Immunol.* 177: 6780–6786.
42. Lepault, F., M. C. Gagnerault, C. Faveeuw, and C. Boitard. 1994. Recirculation, phenotype and functions of lymphocytes in mice treated with monoclonal antibody MEL-14. *Eur. J. Immunol.* 24: 3106–3112.
43. Panther, E., M. Idzko, Y. Herouy, H. Rheinen, P. J. Gebicke-Haerter, U. Mrowietz, S. Dichmann, and J. Norgauer. 2001. Expression and function of adenosine receptors in human dendritic cells. *FASEB J.* 15: 1963–1970.
44. Panther, E., S. Corinti, M. Idzko, Y. Herouy, M. Napp, A. La Sala, G. Girolomoni, and J. Norgauer. 2003. Adenosine affects expression of membrane molecules, cytokine and chemokine release, and the T-cell stimulatory capacity of human dendritic cells. *Blood* 101: 3985–3990.
45. Kalsi, K., C. Lawson, M. Dominguez, P. Taylor, M. H. Yacoub, and R. T. Smolenski. 2002. Regulation of ecto-5′-nucleotidase by TNF-α in human endothelial cells. *Mol. Cell. Biochem.* 232: 113–119.

46. Niemela, J., T. Henttinen, G. G. Yegutkin, L. Airas, A. M. Kujari, P. Rajala, and S. Jalkanen. 2004. IFN-α induced adenosine production on the endothelium: a mechanism mediated by CD73 (ecto-5'-nucleotidase) up-regulation. *J. Immunol.* 172: 1646–1653.
47. Narravula, S., P. F. Lennon, B. U. Mueller, and S. P. Colgan. 2000. Regulation of endothelial CD73 by adenosine: paracrine pathway for enhanced endothelial barrier function. *J. Immunol.* 165: 5262–5268.
48. Mehul, B., M. Dovenmette-Moyne, M. Aubery, H. Mannherz, and P. Codogno. 1990. 5'-Nucleotidase is involved in chick embryo myoblast spreading on laminin. *Cell Biol. Int. Rep.* 2: 155–164.
49. Montesinos, M. C., M. Takedachi, L. F. Thompson, T. F. Wilder, P. Fernández, and B. N. Cronstein. 2007. The anti-inflammatory mechanism of methotrexate depends on extracellular conversion of adenine nucleotides to adenosine by ecto-5'-nucleotidase: findings in a study of ecto-5'-nucleotidase gene-deficient mice. *Arthritis Rheum.* 56: 1440–1445.
50. Grenz, A., H. Zhang, T. Eckle, M. Mittelbronn, M. Wehrmann, C. Köhle, D. Cloor, L. F. Thompson, H. Osswald, and H. K. Eltzschig. Protective role of ecto-5'-nucleotidase (CD73) in renal ischemia. *J. Am. Soc. Nephrol.* 18: 833–845.
51. Volmer, J. B., L. F. Thompson, and M. R. Blackburn. 2006. Ecto-5'-nucleotidase (CD73)-mediated adenosine production is tissue protective in a model of bleomycin-induced lung injury. *J. Immunol.* 176: 4449–4458.
52. Schulte, G., and B. B. Fredholm. 2003. The G_s-coupled adenosine A_{2B} receptor recruits divergent pathways to regulate ERK1/2 and p38. *Exp. Cell Res.* 290: 168–176.
53. Fukuhara, S., A. Sakurai, H. Sano, A. Yamagishi, S. Somekawa, N. Takakura, Y. Saito, K. Kangawa, and N. Mochizuki. 2005. Cyclic AMP potentiates vascular endothelial cadherin-mediated cell-cell contact to enhance endothelial barrier function through an Epac-Rap1 signaling pathway. *Mol. Cell. Biol.* 25: 136–146.
54. Patterson, C. E., H. Lum, K. L. Schaphorst, A. D. Verin, and J. G. Garcia. 2000. Regulation of endothelial barrier function by the cAMP-dependent protein kinase. *Endothelium* 7: 287–308.
55. Linden, J., T. Thai, H. Figler, X. Jin, and A. S. Robeva. 1999. Characterization of human A_{2B} adenosine receptors: radioligand binding, Western blotting, and coupling to G_q in human embryonic kidney 293 cells and HMC-1 mast cells. *Mol. Pharmacol.* 56: 705–713.
56. Herman, P. G., I. Yamamoto, and H. Z. Mellins. 1972. Blood microcirculation in the lymph node during the primary immune response. *J. Exp. Med.* 136: 697–714.
57. Anderson, N. D., A. O. Anderson, and R. G. Wyllie. 1975. Microvascular changes in lymph node draining skin allografts. *Am. J. Pathol.* 81: 131–160.

Periodontal Tissue Regeneration Using Fibroblast Growth Factor -2: Randomized Controlled Phase II Clinical Trial

Masahiro Kitamura[1], Keisuke Nakashima[2], Yusuke Kowashi[2], Takeo Fujii[3], Hidetoshi Shimauchi[4], Takashi Sasano[4], Toshi Furuuchi[4], Mitsuo Fukuda[5], Toshihide Noguchi[5], Toshiaki Shibutani[6], Yukio Iwayama[6], Shogo Takashiba[7], Hidemi Kurihara[8], Masami Ninomiya[9], Jun-ichi Kido[9], Toshihiko Nagata[9], Takafumi Hamachi[10], Katsumasa Maeda[10], Yoshitaka Hara[11], Yuichi Izumi[12], Takao Hirofuji[13], Enyu Imai[14], Masatoshi Omae[15], Mitsuru Watanuki[16], Shinya Murakami[1]*

1 Osaka University Dental Hospital, Suita, Japan, **2** Dental Hospital, Health Sciences University of Hokkaido, Ishikari-Tobetsu, Japan, **3** Medical and Dental Clinic, Health Sciences University of Hokkaido, Sapporo, Japan, **4** Tohoku University Dental Hospital, Sendai, Japan, **5** Aichigakuin University Dental Hospital, Nagoya, Japan, **6** Asahi University Dental Hospital, Mizuho, Japan, **7** Okayama University Hospital of Dentistry, Okayama, Japan, **8** Hiroshima University Hospital of Dentistry, Hiroshima, Japan, **9** Tokushima University Dental Hospital, Tokushima, Japan, **10** Kyushu University Dental Hospital, Fukuoka, Japan, **11** Nagasaki University Hospital, Attached School of Dentistry, Nagasaki, Japan, **12** Kagoshima University Dental Hospital, Kagoshima, Japan, **13** Fukuoka Dental College Hospital, Fukuoka, Japan, **14** Osaka University Hospital, Suita, Japan, **15** Izumisano Municipal Hospital, Rinku General Medical Center, Izumisano, Japan, **16** Kaken Pharmaceutical Co., Ltd., Tokyo, Japan

Abstract

Background: The options for medical use of signaling molecules as stimulators of tissue regeneration are currently limited. Preclinical evidence suggests that fibroblast growth factor (FGF)-2 can promote periodontal regeneration. This study aimed to clarify the activity of FGF-2 in stimulating regeneration of periodontal tissue lost by periodontitis and to evaluate the safety of such stimulation.

Methodology/Principal Findings: We used recombinant human FGF-2 with 3% hydroxypropylcellulose (HPC) as vehicle and conducted a randomized double-blinded controlled trial involving 13 facilities. Subjects comprised 74 patients displaying a 2- or 3-walled vertical bone defect as measured ≥3 mm apical to the bone crest. Patients were randomly assigned to 4 groups: Group P, given HPC with no FGF-2; Group L, given HPC containing 0.03% FGF-2; Group M, given HPC containing 0.1% FGF-2; and Group H, given HPC containing 0.3% FGF-2. Each patient underwent flap operation during which we administered 200 μL of the appropriate investigational drug to the bone defect. Before and for 36 weeks following administration, patients underwent periodontal tissue inspections and standardized radiography of the region under investigation. As a result, a significant difference ($p = 0.021$) in rate of increase in alveolar bone height was identified between Group P (23.92%) and Group H (58.62%) at 36 weeks. The linear increase in alveolar bone height at 36 weeks in Group P and H was 0.95 mm and 1.85 mm, respectively ($p = 0.132$). No serious adverse events attributable to the investigational drug were identified.

Conclusions: Although no statistically significant differences were noted for gains in clinical attachment level and alveolar bone gain for FGF-2 groups versus Group P, the significant difference in rate of increase in alveolar bone height ($p = 0.021$) between Groups P and H at 36 weeks suggests that some efficacy could be expected from FGF-2 in stimulating regeneration of periodontal tissue in patients with periodontitis.

Trial Registration: ClinicalTrials.gov NCT00514657

Citation: Kitamura M, Nakashima K, Kowashi Y, Fujii T, Shimauchi H, et al. (2008) Periodontal Tissue Regeneration Using Fibroblast Growth Factor -2: Randomized Controlled Phase II Clinical Trial. PLoS ONE 3(7): e2611. doi:10.1371/journal.pone.0002611

Editor: William Giannobile, University of Michigan, United States of America

Received September 10, 2007; **Accepted** May 13, 2008; **Published** July 2, 2008

Funding: This study was supported by Kaken Pharmaceutical Co., Ltd., which proposed study protocol and was responsible for data collection and prespecified statistical analysis. Preparation of the manuscript was consigned to the authors and the views expressed in this article do not necessarily reflect those of Kaken Pharmaceutical Co., Ltd.

Competing Interests: SM received research grants from Kaken Pharmaceutical Co., Ltd. MW is an employee and stockholder of Kaken Pharmaceutical Co., Ltd.

* E-mail: ipshinya@dent.osaka-u.ac.jp

Introduction

Periodontitis, evoked by the bacterial biofilm (dental plaque) that forms around teeth, progressively destroys the periodontal tissue supporting the teeth, including the periodontal ligament, cementum, alveolar bone and gingiva. Ultimately, this chronic inflammatory disease can lead to loss of the affected teeth [1–3]. All over the world, this disease remains highly prevalent [4] and is considered to threaten quality of life (QOL) for middle-aged and older populations as far as "oral" functions are concerned. Some

success has been achieved in suppressing progression of periodontitis by mechanically removing bacterial biofilm, the very cause of the disease. However, removal of the cause, bacterial plaque, with conventional periodontal and/or surgical treatments can, at best, reduce pocket depth and diminish inflammation in the affected region. No such treatment can ever regenerate lost periodontal tissue or normal structure and functionality. Considering that the "mouth" and "teeth" have various aesthetic and functional roles to play, establishing a brand-new treatment that enables the regeneration and rebuilding of periodontal tissue once destroyed by periodontal disease represents a task of tremendous importance.

To regenerate periodontal tissue destroyed by periodontitis, the chain of events requires stimulation of cementoblasts and osteoblasts into differentiation on the dental root and alveolar bone surfaces facing the region of periodontal tissue defect, followed by regeneration of the cementum and alveolar bone. Collagen fascicles produced by the periodontal ligament fibroblasts should then be embedded into those regenerated hard tissues, to rebuild new tissue to support teeth. Researchers have recently confirmed the existence of mesenchymal stem cells within the periodontal ligament, one of the cornerstones of periodontal tissue. These stem cells can differentiate into cells such as cementoblasts and osteoblasts [5]. Using the biological potentials of those stem cells to stimulate the regeneration of periodontal tissue is now being recognized as clinically possible. Some researchers are already trying to establish new treatments to accelerate the regeneration of periodontal tissue by local application of human recombinant cytokines to stimulate proliferation and differentiation into hard-tissue forming cells of undifferentiated mesenchymal cells among periodontal ligament cells. Direct local application of a combination of factors such as platelet-derived growth factor (PDGF) and insulin-like growth factor (IGF)-I [6], bone morphogenetic protein (BMP)-2 [7,8], transforming growth factor (TGF)-β [9], osteogenic protein (OP)-1 [10] and brain-derived neurotrophic factor (BDNF) [11] to artificial defects in periodontal tissue made in laboratory animals reportedly stimulates and promotes regeneration of regional periodontal tissue. In addition, the efficacy of PDGF-BB plus β-tricalcium phosphate (β-TCP, an osteoconductive scaffold) for periodontal tissue regeneration in human has recently been reported [12].

Fibroblast growth factor (FGF)-2 displays potent angiogenic activity and mitogenic ability on mesenchymal cells. To date, FGF-2 has been reported as efficacious in regenerating periodontal tissue in models of artificial defect of periodontal tissue in beagles and non-human primates (*Macaca fascicularis*) and in a model of surgically created periodontitis in beagles [13–15].

The present clinical trial used hydroxypropylcellulose (HPC)-based FGF-2 as the investigational agent. The purpose of this trial was to both clarify the activity of FGF-2 to regenerate periodontal tissue in periodontitis patients and to confirm drug safety. This study was a randomized, double-blinded clinical trial (Phase II) involving placebos and multiple dental facilities in compliance with good clinical practice (GCP) guidelines, representing the first trial to examine the efficacy and safety of FGF-2 in periodontitis patients with concurrent control of dose-response relationships.

The periodontium that supports teeth displays a tissue structure wherein the alveolar bone (hard tissue surrounding dental roots) is covered by the gingiva (soft tissue), and "true regeneration" thus involves the regeneration of both hard and soft tissues. To improve tooth support, regenerating hard tissues including alveolar bone is crucial. Hence, in the present study, under the assumption that FGF-2 would regenerate both hard and soft tissues, the rate of increase in alveolar bone height was established as the most important outcome measure. Furthermore, to confirm soft-tissue regeneration, the millimeter of clinical attachment level (CAL) regained was added as a main outcome measure.

Including recruitment of subjects, the clinical trial was performed from December 1, 2001 to September 29, 2004.

Methods

The Protocol for this trial and supporting CONSORT checklist are available as supporting informations; see Checklist S1 and Protocol S1.

This was a randomized, double-blinded, clinical trial of dose responses including placebo comparison, involving 13 dental facilities. Study protocols were approved prior to initiation of the study by the institutional review boards of the respective participating facilities.

1. Participants

Patients with periodontitis visiting any of the 13 dental institutions listed in Table 1 were requested to participate. In compliance with GCP guidelines, prospective 91 patients who provided written informed consent underwent clinical inspection and oral cavity diagnosis. Among 91 patients 80 patients who satisfied the selection and exclusion criteria described in Tables 2 and 3 were finally registered. Each subject received a standard initial preparation, including oral hygiene instruction, full-mouth scaling and root planing before surgical treatment, to minimize bacterial insult and reduce variability between lesions at baseline. Using oral radiographs and periodontal tissue inspection results, regions of investigation were determined as 2- or 3-walled vertical periodontal tissue defects ≥3 mm apical to the remaining alveolar bone crest.

2. Interventions, Design and Procedure

This trial employed recombinant human FGF-2 (Code No. KCB-1; Kaken Pharmaceutical Co., Ltd., Tokyo, Japan) produced by genetic recombination that introduced the gene for human FGF-2 into *Escherichia coli*. To improve the operability of drug administration to the region of alveolar bone defect, before administration we mixed freeze-dried FGF-2 with 3% HPC, a colorless and viscid solution, and prepared the gel-like investigational drug for this clinical trial (Code No. KCB-1D). FGF-2 concentration in the investigational drug was then prepared to 0% (placebo), 0.03%, 0.1% or 0.3% and administered to the region of investigation within 2 h of preparation. Before the start and after completion of investigational drug administration, a third-party organization (University of Shizuoka, Shizuoka, Japan) measured FGF-2 concentrations for each group to ascertain that FGF-2 concentrations in vials were accurate according to good manufacturing practice standards.

The clinical trial was conducted according to the schedule shown in Figure 1. The 80 patients were registered at the Registration Center (Adjust Co., Ltd., Sapporo, Japan) and then randomly assigned to the following 4 groups: Group P, placebo group administered HPC containing no FGF-2; Group L, administered HPC containing 0.03% FGF-2; Group M, administered HPC containing 0.1% FGF-2; and Group H, administered HPC containing 0.3% FGF-2.

All flap operations were performed in accordance with the modified Widman procedure. The proposed surgical area was anesthetized using local anesthetic. Following intracrevicular incision, buccal and lingual full-thickness (mucoperiosteal) flaps were elevated. Following reflection of the mucoperiosteal flap, all granulation tissue associated with the bone defect was removed. Subgingival soft and hard deposits on the root surface were

Table 1. The 13 trial dental facilities and the investigators

Trial facilities	Investigators	Number of patients
Dental Hospital, Health Sciences University of Hokkaido	Yusuke Kowashi	4
Medical and Dental Clinic, Health Sciences University of Hokkaido	Takeo Fujii	9
Tohoku University Dental Hospital	Hidetoshi Shimauchi	6
Aichigakuin University Dental Hospital	Mitsuo Fukuda	7
Asahi University Dental Hospital	Toshiaki Shibutani	6
Osaka University Dental Hospital	Masahiro Kitamura	6
Okayama University Hospital of Dentistry	Shogo Takashiba	11
Hiroshima University Hospital of Dentistry	Hidemi Kurihara	3
Tokushima University Dental Hospital	Jun-ichi Kido	12
Kyushu University Dental Hospital	Takafumi Hamachi	2
Nagasaki University Hospital Attached School of Dentistry	Yoshitaka Hara	6
Kagoshima University Dental Hospital	Yuichi Izumi	8
Fukuoka Dental College Hospital	Takao Hirofuji	0
		80

doi:10.1371/journal.pone.0002611.t001

removed utilizing both hand and ultrasonic instrumentation to ensure thorough degranulation and root planing. After that, 200 μL of investigational drug was administered to the bone defect region described above. No specific root conditioning was performed.

Next, at 1, 2 and 4 weeks after administration, the same clinical inspections were performed as before administration, and anti-FGF-2 antibodies in serum 2 and 4 weeks after administration were measured. At 12, 24 and 36 weeks following administration, standardized radiographs were taken, periodontal tissues were inspected and subjective symptoms and objective findings were observed. In addition, 6 patients from each of the groups were randomly selected and blood samples were drawn. At 1, 2 and 4 h after administering the investigational drug, FGF-2 concentrations in serum were measured.

3. Randomization

An independent organization, the Registration Center (Adjust Co., Ltd., Sapporo, Japan), was used to keep treatment allocation inaccessible to any patients or other individuals involved in the trial. The Registration Center created an allocation table in which a block size of 4 cases per block was allocated to investigational drugs comprising placebo (Group P), 0.03% FGF-2 (Group L), 0.1% FGF-2 (Group M) or 0.3% FGF-2 (Group H). According to this allocation table, a label indicating the corresponding drug number was attached to each and every vial of drug. After drugs were allocated, the Registration Center sealed and kept the allocation table in confidence until the clinical trial was completed. Freeze-dried drugs for Groups P, L, M and H were indistinguishable based on appearance.

Investigators at each facility checked all inclusion and exclusion criteria and registered patients one at a time by faxing patient information obtained under informed consent to the Registration Center. The center again checked the documents to make sure that each subject had satisfied all inclusion and exclusion criteria, then randomly allocated subjects as necessary to receive drugs based on a single block consisting of one drug sample each from Groups P, L, M, and H. The assigned drug numbers were then faxed back to the investigators. The blind was not broken until this clinical trial was completely finished.

Table 2. Criteria for selecting subjects

1)	Those diagnosed as having, from radiography and other results, 2- or 3-walled vertical intrabony defect as being measured at ≥3 mm apical to the remaining alveolar bone crest
2)	Those who have accomplished initial preparation and have been showing good compliance
3)	Those with mobility of the tooth to investigate of Degree 2 or less and with width of attached gingiva for which the existing Guided Tissue Regeneration (GTR) treatment is considered appropriate (Those with no width of keratinized gingival is not eligible)
4)	Those for whom supportive periodontal treatment (SPT) is applicable, in accordance with usual post-operative procedures following flap operation and GTR treatment
5)	Those whose oral hygiene is well established and who are able to perform appropriate tooth brushing following instructions of the investigators and/or sub-investigators after investigational drug administration
6)	Those ≥20-years-old and <65-years-old
7)	Those who understand the purposes of the trial and are capable of making an independent decision to comply with trial requirements
8)	Those who are able to visit their hospitals in accordance with the trial schedule

We selected those patients who met the criteria listed above, from those who the investigators and/or sub-investigators determined were in need of flap operation.

doi:10.1371/journal.pone.0002611.t002

Table 3. Criteria for excluding subjects

1)	Those administered a calcium antagonist during the 4 weeks preceding administration of the investigational drug
2)	Those in need of administration of adrenal cortical steroid (equivalent to>20 mg/day of Predonin) within 4 weeks after investigational drug administration
3)	Those scheduled to undergo a surgical operation in the vicinity of the tooth to investigate within 36 weeks after investigational drug administration
4)	Those with coexisting mental or consciousness disorder
5)	Those with coexisting malignant tumour or history of the same
6)	Those with coexisting diabetes (HbA_{1C} >6.5%)
7)	Those in an extremely poor nutritional condition (serum albumin concentration <2 g/dL)
8)	Those with ≥200 mL of blood drawn during the 4 weeks preceding investigational drug administration
9)	Those administered another investigational drug during the 24 h preceding investigational drug administration
10)	Those with coexisting disorder of the kidney, liver, blood and/or circulatory system (Grade 2 or above)
11)	Those who are either pregnant, possibly pregnant or breast-feeding, or who hope to become pregnant during the period of the trial
12)	Those with a previous history of hypersensitivity to a protein drug
13)	Others who the investigators or sub-investigators determined as unsuitable for the trial

doi:10.1371/journal.pone.0002611.t003

4. Outcome measures

Main outcome measures prespecified in the study protocol comprised: rate of increase in alveolar bone height; and millimeter of CAL regained. In addition, we examined whether and to what extent adverse events emerged for which causal relationships with the investigational drug were not ruled out before breaking the blind. We set rate of increase in alveolar bone height as the most statistically important outcome (primary outcome). Probing depth (PD), bleeding on probing (BOP), gingival index (GI), tooth mobility (MO), gingival recession (REC), plaque index (PII), and width of keratinized gingiva (KG) were selected as secondary outcome measures.

1) Standardized radiography for regions of investigation

Our geometrically standardized radiography employed dental film (Kodak InSight Super Poly-Soft; Eastman Kodak Company, New York, USA) and photograph indicators (Cone Indicator-II; Hanshin Technical Laboratory, Nishinomiya, Japan) customized with resin stents.

Five doctors specializing in dental radiology from the Department of Oral Diagnosis at Tohoku University Graduate School of Dentistry independently measured rate of increase in alveolar bone height using the methods described in Figure 2. Errors caused by slight variation in angulations of X-ray imaging were corrected based on the distance between two immobile anatomical

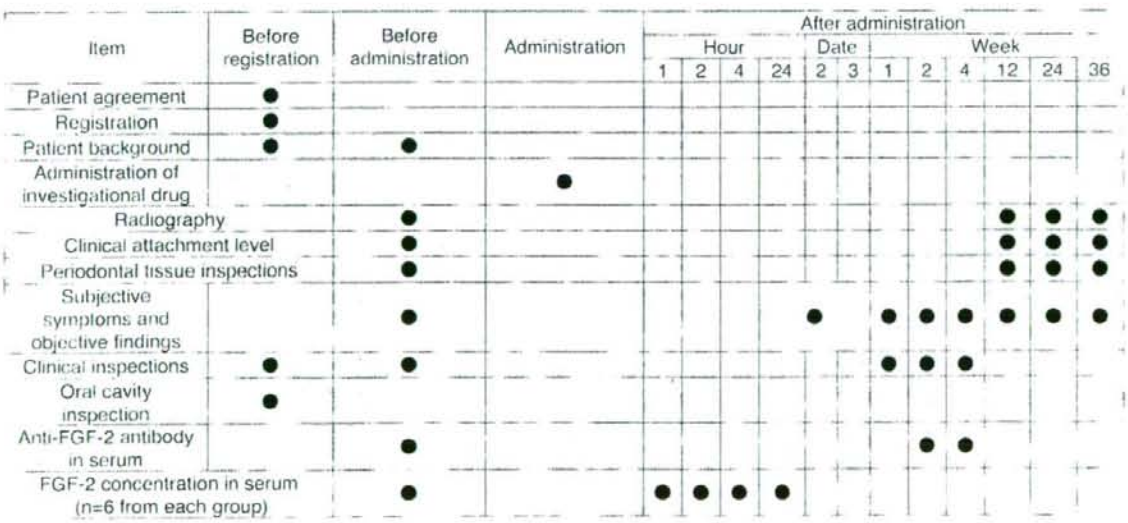

Figure 1. Schedule of the clinical trial. We randomly allocated the 80 patients into 4 groups (n = 20 each): 1) a placebo group (Group P); 2) a group administered 0.03% FGF-2 (Group L); 3) a group administered 0.1% FGF-2 (Group M); and 4) a group administered 0.3% of FGF-2 (Group H). The clinical trial was then conducted in accordance with the clinical trial schedule. We also measured FGF-2 concentrations in the blood serum of 6 patients randomly chosen from each of the 4 groups, before and then 1 h, 2 h and 4 h after administration of the investigational drug.
doi:10.1371/journal.pone.0002611.g001

reference points. The median of 5 measurements taken from the same image was then selected for efficacy analysis. Before making measurements in the present study, X-ray images were read to measure intra- and interexaminer variations. Each of the 5 doctors measured the same sample 5 times to calculate coefficients of variation. The results showed that intra- and interexaminer coefficients of variation were both 3%, confirming the absence of marked variations.

2) Inspection of periodontal tissue around the tooth under investigation

We measured the items shown in Table 4 at 6 positions (mesiobuccal, buccal, distobuccal, mesiolingual, lingual and distolingual) around each tooth under investigation.

All examiners used PCP-UNC-15 periodontal probes (Hu-Friedy, Chicago, IL). We held meetings with each investigator from all of the participating facilities. In addition, a start-up meeting in which all investigators from a single facility participated was held at each facility. In these meetings, the protocol for this clinical trial was confirmed and clinical evaluations were standardized between facilities. In all facilities, the same person (MW) explained the detailed methods of probing inspections to all investigators and confirmed reproducibility and consistency for each investigator. Furthermore, prior to initiating baseline measurements, intra- and interexaminer calibrations were performed on patients at each facility to ensure reproducibility and consistency by each investigator. Each patient was examined by the same examiner at every recall visit throughout this clinical trial.

5. Safety evaluation

1) Observation of subjective symptoms and objective findings

Medical findings for both the oral cavity and whole body were confirmed by interview and visual inspection.

2) Clinical inspections

A clinical testing company (SRL Medisearch Inc., Tokyo, Japan) measured the inspection items (see Table S1 of supporting items). In cases where we discovered unusual changes in any of the clinical inspection values listed within 4 weeks after administration of the investigational drug, a follow-up survey was conducted.

3) Measurement of anti-FGF-2 antibody levels in serum

The Pharmacokinetics Department of Kaken Pharmaceutical Co., Ltd. measured levels of anti-FGF-2 antibody (IgG) in serum using ELISA.

4) Measurement of FGF-2 concentration within serum

The Metabolism Research Department of Kaken Pharmaceutical Co., Ltd. measured FGF-2 concentrations in serum using ELISA.

6. Sample size calculation

The effect of a combination drug comprising recombinant human PDGF-BB and IGF-I in humans on periodontal regeneration has already been reported [19]. In PDGF-BB/IGF-I-treated subjects (n = 16), mean (±standard error of mean) bone fill was 18.5±7% for control sites (surgery alone) and 42.3±9% for PDGF-BB/IGF-I sites with a mean difference of 23.8%. Assuming a rate of increase for placebo control of 20% (standard deviation, 28%) in alveolar bone of the defect region, the planned sample size

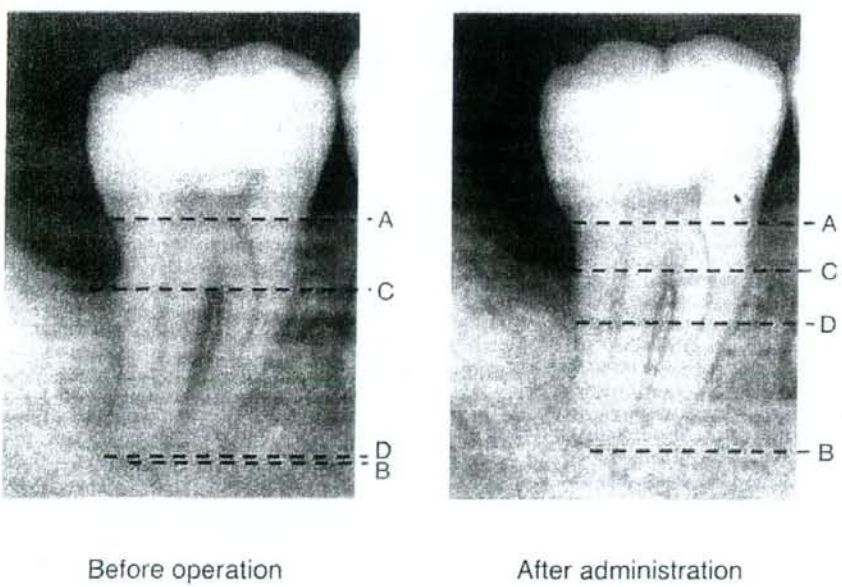

Figure 2. Measured points of alveolar bone height using standardized radiographs. Standardized dental radiographs taken before and after FGF-2 administration in one subject (a 29-year-old man) given 0.3% FGF-2. Points A, B, C and D represent the cementoenamel junction, apex, remaining alveolar bone crest and bottom of the bone defect, respectively. The examiners measured tooth axis heights between Points A and B, Points A and C, and Points A and D on the X-ray for each patient. To adjust for slight errors due to imaging, measurements for 5 examiners were multiplied by A-B ratio of before to after administration to correct A-B, A-C and A-D after administration (adjusted A-B, A-C and A-D, respectively). Rate of increase in alveolar bone height was derived from the following calculation formula. [(A-D before administration) - (adjusted A-D after administration)] by C-D before administration. On this radiography, C-D before administration, A-D before administration and, adjusted A-D after administration measured 9.00 mm, 12.80 mm and 5.93 mm, respectively. These values assigned to the above formula, we obtained the rate of increase in alveolar bone height as follows. The rate of increase in alveolar bone height (%) = 100(12.80–5.93)/9.00 = 76.35.
doi:10.1371/journal.pone.0002611.g002

Table 4. Periodontal tissue inspection

1)	Clinical attachment level (CAL): A stent was prepared for each subject. Using as the control point the cementoenamel junction or margin of the restorative material, distance between the control point and bottom of the gingival sulcus was measured for each test subject, using the same periodontal probe.
2)	Probing depth (PD): Simultaneously with CAL measurement, we measured distance from the gingival margin to the bottom of the gingival sulcus for each subject using the same periodontal probe.
3)	Bleeding on probing (BOP; + or −): The presence of bleeding was checked 10 s after probing.
4)	Gingival index (GI): GI was determined as described by Löe and Silness.[16]
5)	Mobility of tooth (MO): MO was determined as described by Miller.[17]
6)	Recession of gingiva (REC): Using as the control point the cementoenamel junction or margin of the restorative material, distance between the control point and gingival margin was measured for each subject, using the same periodontal probe.
7)	Plaque index (PII): PII was determined as described by Silness and Löe.[18]
8)	Width of keratinized gingiva (KG): The shortest distance between the coronal gingival margin and mucogingival junction was measured for each subject, using the same periodontal probe.

doi:10.1371/journal.pone.0002611.t004

of 20 patients in each group would provide 90% power to detect any clinically relevant treatment difference of 30% at a two-tailed significance level of 0.05.

7. Statistical methods

For analysis, we employed SAS version 8.2 software (SAS Institute Inc., Carey, North Carolina, USA). The level of statistical significance was set at $p<0.05$ in advance. Data analysis covered those patients administered the randomly allocated investigational drugs. In analyses concerning efficacy, those patients found to have either 1- or 4-walled intrabony defect during surgery after allocation were excluded. To statistically compare the 3 dose groups in terms of rate of increase in alveolar bone mass with the placebo group, the Dunnett option was used based on the Mixed procedure in the SAS system, in which adjusted p-values were computed for multiple comparisons, and analysis for rates of increase during follow-up was performed using repeated-measures analysis of variance with the Mixed procedure.

Results

1. Patient characteristics at the beginning of the trial (baseline characteristics)

Figure 3 shows flow of patients through the study. The 91 patients screened as subjects were consenting periodontitis patients for whom periodontal tissue regeneration therapy was indicated by investigators based on these criteria among a large number of potential subjects. Following the exclusion of 11 of these 91 patients, a final total of 80 patients were enrolled as subjects in the present clinical trial. The 11 patients were excluded due to findings on clinical inspection that could not have been determined by investigators during clinical periodontal diagnosis, or due to withdrawal of consent to participate. The 80 patients were then randomly assigned to 4 groups of 20 patients each. Table 5 shows the baseline characteristics of patients.

2. Evaluation of efficacy

Rate of increase in alveolar bone height at 12, 24 and 36 weeks after FGF-2 administration are shown in Table 6. A significant difference ($p=0.021$) was only identified between Group P and Group H at 36 weeks. The detailed data at 36 weeks are shown in Fig. 4 and Table 7. Adjusted mean differences from Group P were also calculated as least square mean (LSMean) differences based on two-way analysis of variance or analysis of covariance (data not shown). Adjusted mean differences for gender, site of investigational drug administration (maxilla or mandible), CAL, REC, GI, MO, PII and type of bone defect mostly resembled raw mean differences and the lower 95% confidence limits of LSMean difference (Group P vs. H) was above zero (0<lower 95% confidence limit). These results indicate that baseline characteristic imbalances between groups had no influence on evaluation of efficacy. Regarding the CAL regained (Table 8), REC, KG, MO and PII (see Table S2 of supporting items), no significant differences existed between the 4 groups. Although PD, GI and BOP prevalence all decreased with time following periodontal surgical treatment in the 4 groups (see Table S3 of supporting items), no significant differences were noted between these groups.

Two-way analysis of variance was used to assess facility differences in the 4 groups in the rate of increase in alveolar bone height, revealing no significant treatment-by-facility interaction ($p=0.795$). This suggests that no marked facility differences existed with respect to response.

3. Safety evaluation

Major adverse events for which causal relationships with the investigational drug were not ruled out before breaking the blind included positive urinary albumin, increased urinary excretion of β2-microglobulin and N-acetyl-beta-D-glucosamidase, increased serum creatine kinase and C-reactive protein and increased cases of hypersensitive dentine (see Table S4 of supporting items). Frequencies of these adverse events were independent of FGF-2 concentration. No serious adverse events were observed throughout the clinical trial period. A possible association was also considered between frequency of adverse events observed during the trial and the investigational drug administration. None of the adverse events exhibited a strong causal relationship or were severe, and except for one case, all events resolved without any special treatment. For each group, the presence/absence and frequency of adverse events were calculated. Fisher's exact test showed that group allocations exhibited no association to the presence/absence of adverse events ($p=0.469$). In addition, during the inspection following FGF-2 administration (Fig. 1), no FGF-2 or anti-FGF-2 antibodies were detected in the serum of any patients.

Discussion

Originally isolated from bovine hypophysis in the 1970s, FGF-2 is a protein with a molecular weight of 17,000 that acts to promote proliferation of fibroblasts. Researchers have isolated, refined and

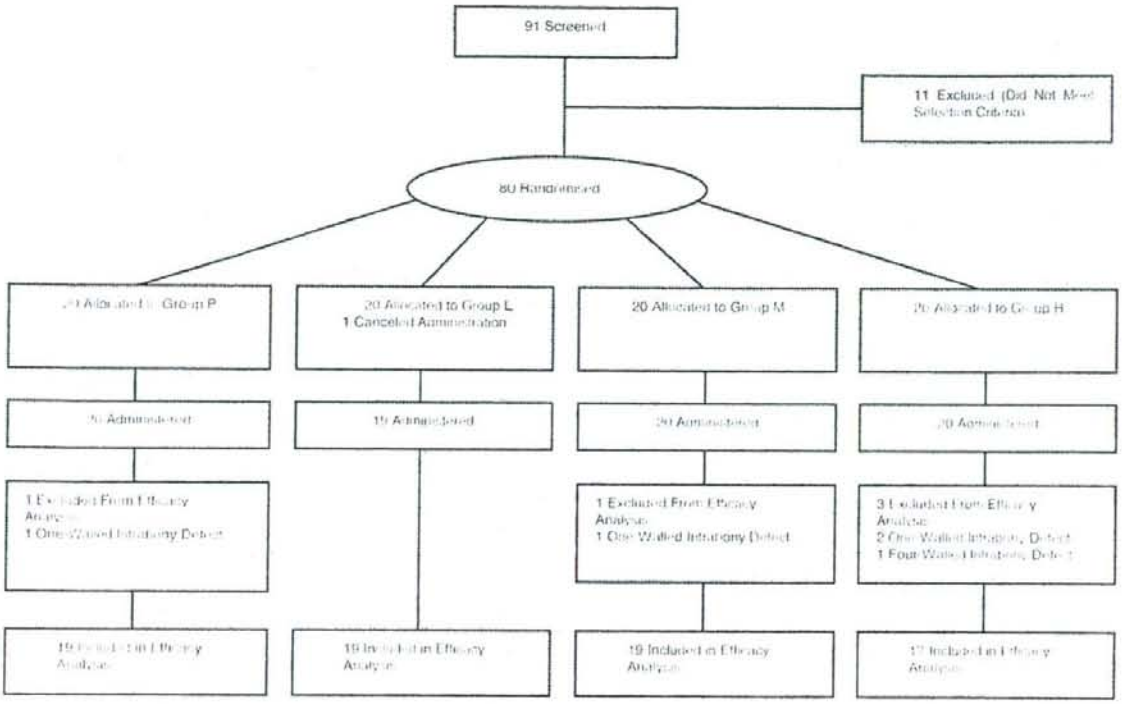

Figure 3. Flow of patients through the study.
doi:10.1371/journal.pone.0002611.g003

genetically cloned human FGF-2 to clarify numerous different biological activities of the protein. As yet, many studies have reported that FGF-2 stimulates proliferation of numerous kinds of cells, including not just fibroblasts, but also vascular endothelial, vascular smooth muscle, neuroectodermal, osteoblast, cartilage and epidermal cells. The protein is now known to be deeply involved in cell proliferation and differentiation and also in control of extracellular matrix generation during the processes of tissue generation and wound healing [20–25]. Many recent reports in the field of regenerative medicine have described the use of cytokines as "signaling molecules", stimulating adequate proliferation and differentiation of tissue stem cells. Among those cytokines, FGF-2 is winning attention from researchers due to activity in promoting proliferation of mesenchymal stem cells while maintaining multilineage potential [6]. The protein has already been utilized in a human intractable ulcer-curing drug (Fiblast Spray; Kaken Pharmaceutical Co., Ltd.) for more than 4 years.

We have already studied the stimulation of periodontal tissue regeneration by FGF-2 in animal models and believe that the protein represents a major candidate for a periodontal tissue-regenerating agent. This is based on stimulation of proliferation for both kinds of cell groups that rebuild hard and soft tissues along with strong angiogenic activity, which is indispensable in tissue regeneration. Animal tests have revealed that in artificial models of periodontal tissue defect in beagles [13,15] and non-human primates (*M. fascicularis*) [14], FGF-2 significantly stimulates neogenesis of alveolar bone, periodontal ligament and cementum, without invoking abnormal effects such as down-growth of the gingival epithelia, resorption of the dental root or ankylosis.

Based on effective concentrations of FGF-2 for periodontal tissue regeneration in animal trials, in addition to the results of our Phase I trial in which FGF-2 was administered intravenously to healthy adult humans, we determined the concentrations and doses administered to periodontal regions of patients in the present clinical trial. More specifically, the results of testing with artificial defect models of periodontal tissue in beagles led us to estimate that an effective FGF-2 concentration for stimulation of periodontal tissue regeneration was 0.03–0.3%. This range of concentrations was therefore applied in the present clinical trial. We selected 200 μL as the dose, considering that this was good enough to work on the defect region of periodontal tissue. In addition, preclinical trial results have suggested that the maximum quantity of administered FGF-2 to enter the circulation in the present trial herein would be around 1.2 mg/body, less than the 30 mg/body for which safety was confirmed in our Phase I trial. The 91 patients screened as subjects and a final total of 80 patients were enrolled as subjects. The patient characteristics were almost similar among groups. However, we understand that we could not perfectly eliminate biasing influences of patient characteristics in this study and a larger scale trial is needed in the future.

In evaluating efficacy, we surveyed 74 cases of 2- or 3-walled intrabony defect that satisfied the selection criteria. To evaluate periodontal tissue regeneration, evaluating fibrous attachment accompanied by neogenesis of alveolar bone and cementum is important. Rate of increase in alveolar bone height observed in close proximity to the dental root was measured as a prespecified primary outcome in this clinical trial.

Use of 0.3% FGF-2 stimulated 58.6% regeneration, which was at least comparable with the previous results within 9 months after

Table 5. Patient characteristics

Item	Classification	Group P	Group L	Group M	Group H
Numbers of patients		20	19	20	20
Sex (% of patients)	Male	55.0	36.8	25.0	35.0
	Female	45.0	63.2	75.0	65.0
Age (years)	Mean (SD)	49.2 (8.9)	46.2 (11.1)	46.8 (10.3)	47.7 (10.5)
Coexisting disease (% of patients)	No	70.0	57.9	75.0	85.0
	Yes	30.0	42.1	25.0	15.0
Previous history	No	75.0	73.7	60.0	60.0
	Yes	25.0	26.3	40.0	40.0
Smoking habit	No	75.0	89.5	80.0	70.0
	Yes	25.0	10.5	20.0	30.0
Region of administration (Major classification) (% of patients)	Maxilla	40.0	57.9	55.0	60.0
	Mandible	60.0	42.1	45.0	40.0
Region of administration (Minor classification) (% of patients)	Anterior tooth	25.0	21.1	25.0	30.0
	Premolar	35.0	42.1	40.0	40.0
	Molar	40.0	36.8	35.0	30.0
Depth of bone defect at operation (mm)	Mean (SD)	4.7 (1.5)	4.8 (2.4)	4.6 (1.7)	5.7 (2.6)
Classification of bone defect (% of patients)	1-walled	5.0	0.0	5.0	10.0
	2-walled	50.0	47.4	70.0	50.0
	3-walled	40.0	47.4	25.0	30.0
	4-walled	0.0	0.0	0.0	5.0
	2/3-walled	0.0	5.3	0.0	5.0
	1/2-walled	5.0	0.0	0.0	0.0
Treatment to tooth of investigation (% of patients)	No	60.0	57.9	55.0	55.0
	Yes	40.0	42.1	45.0	45.0
Existent of dental pulp (% of patients)	No	15.0	15.8	20.0	25.0
	Yes	85.0	84.2	80.0	75.0
Clinical attachment level (mm)	Mean (SD)	9.3 (2.2)	8.4 (2.7)	8.4 (2.8)	8.3 (3.0)
Probing depth (mm)	Mean (SD)	5.7 (1.2)	5.4 (1.6)	5.1 (2.0)	5.8 (1.7)
Recession (mm)	Mean (SD)	2.4 (1.8)	2.1 (1.5)	2.2 (2.3)	1.7 (1.5)
Width of keratinized gingival (mm)	Mean (SD)	4.9 (2.1)	4.3 (1.9)	4.5 (2.2)	5.3 (2.7)
Gingival bleeding index (% of patients)	−	10.0	15.8	20.0	5.0
	+	90.0	84.2	80.0	95.0
Gingival index (% of patients)	0	35.0	21.1	25.0	10.0
	1	30.0	47.4	40.0	45.0
	2	35.0	31.6	35.0	45.0
Mobility of tooth (% of patients)	0	65.0	57.9	50.0	40.0
	1	35.0	36.8	50.0	55.0
	2	0.0	5.3	0.0	5.0
Plaque index (% of patients)	0	50.0	42.1	80.0	60.0
	1	35.0	57.9	20.0	30.0
	2	15.0	0.0	0.0	10.0

doi:10.1371/journal.pone.0002611.t005

regenerative therapy [19,26,27]. However, no significant difference was identified between Groups P and H in terms of millimeter increments ($p = 0.132$). To confirm the efficacy of the investigational drug using more conventional methods, data in both % and millimeter increments were used to calculate sample size for the next late Phase II trial. In addition, the minimum clinically effective dose will need to be assessed and determined in a future clinical study involving more patients.

Interestingly, no significant difference was observed between the 4 groups in the millimeter of CAL regained, with all groups scoring around 2 mm (see Table S2 of supporting items). The CAL regained following periodontal surgery is derived from the sum of epithelial and fibrous attachments. If periodontal tissue regeneration accompanied by neogenesis of the alveolar bone and cementum is stimulated, fibrous attachment reproducing the natural anatomical morphology is achieved. However, the

Table 6. Changes with time in alveolar bone height

		Group P (n = 19)	Group L (n = 19)	Group M (n = 19)	Group H (n = 17)
rate of increase (%)	12 weeks	6.90 (20.12)	2.03 (18.79)	−0.82 (33.1)	13.86 (33.03)
	24 weeks	17.44 (28.48)	12.33 (27.50)	12.59 (23.67)	35.58 (40.35)
	36 weeks	23.92 (27.52)	20.19 (38.09)	29.39 (37.71)	*58.62 (46.74)
millimeter increase	12 weeks	0.28 (0.80)	0.07 (0.58)	0.15 (0.71)	0.55 (1.37)
	24 weeks	0.67 (1.25)	0.38 (0.97)	0.53 (0.71)	1.21 (1.57)
	36 weeks	0.95 (1.26)	0.54 (1.26)	1.06 (1.16)	1.85 (1.75)

Mean and standard deviations are shown. *A significant difference ($p = 0.021$) was only identified between Group P and Group H at 36 weeks in rate of increase in alveolar bone height.

doi:10.1371/journal.pone.0002611.t006

majority of CAL acquisition following conventional periodontal surgery has been shown to be due to epithelial attachment unaccompanied by alveolar bone regeneration [28–31]. We have previously conducted an animal study using non-human primates and reported that at the FGF-2 administration site, down-growth of gingival epithelial cells was suppressed to achieve fibrous attachment accompanied by neogenesis of the alveolar bone and cementum [14]. In the present study, no significant differences in CAL regained were seen between Group P (conventional periodontal surgery) and the three FGF-2 groups (Table 8). Based on the results of the above-mentioned preclinical study, we deduce that differences may exist between Group P and the three FGF-2 groups in histological ratio of fibrous and epithelial attachments achieving CAL acquisition. Confirmation of the nature of healing tissue requires histological evaluation in a future study.

PD, BOP, GI, MO, REC and KG are generally used to assess pathology in periodontal disease. These parameters do not directly assess the efficacy of FGF-2 in periodontal tissue regeneration, and were selected in the present study as secondary outcome measures to ascertain whether FGF-2 would cause abnormal periodontal healing following periodontal surgery. The fact that no significant

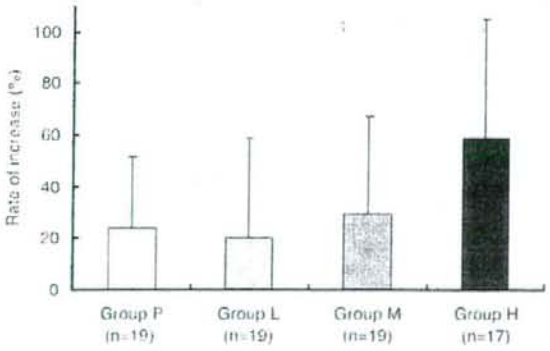

Figure 4. Rates of increase in alveolar bone height in cases of 2- and 3-walled intrabony defects. We compared rates of increase in alveolar bone height at 36 weeks after FGF-2 administration among Group P (19 placebo cases), Group L (19 cases administered 0.03% FGF-2), Group M (19 cases administered 0.1% FGF-2) and Group H (17 cases administered 0.3% FGF-2). This figure shows mean increase rates (%) and standard deviations of alveolar bone height. While no significant difference was observed between Groups L and M and P, Group H showed significantly increased ($p = 0.021$) alveolar bone height in the bone defect region compared to Group P.

doi:10.1371/journal.pone.0002611.g004

differences among these secondary outcome measures for the 4 groups showed that FGF-2 administration did not cause abnormal healing of periodontium following periodontal surgery. Furthermore, frequency of PD, GI, and BOP all dropped over time in all groups after periodontal surgical treatment. These findings show that we can expect FGF-2 administration to provide a therapeutic process similar to that of the conventional flap operation, in addition to the healing outcome of periodontal tissue regeneration. Yet another observation was the lack of recognisable difference in changes to REC and KG, which accompanies periodontal surgical treatment, between Group P and the other 3 groups receiving FGF-2 administration. This confirms that FGF-2 administration does not cause peculiar gingival recession or reduce keratinized gingiva. PII offers a parameter for assessing the amount of plaque causing periodontal disease, and since the degree of plaque deposition can affect the prognosis of periodontal surgery, this parameter was also selected as a secondary outcome measure. In this clinical study, no significant intergroup differences were seen in PII. Moreover, radiography was performed for 67 patients who willingly and positively responded to our "recall" for imaging between week 83 and 132 (inclusive) after administration of investigational drugs (Group P, n = 19; Group L, n = 15; Group M, n = 18; Group H, n = 16). Among these 67 patients, no cases suggested an abnormal increase in alveolar bone exceeding the cementoenamel junction or an equivalent control point or ankylosis (data not shown).

The periodontal ligament comprises heterogenous cell populations and researchers have predicted the existence of some progenitor cells that can differentiate into cementoblasts or osteoblasts [32–34]. A recent study reported that some cells within the ligament express STRO-1 and CD146 mesenchymal stem cell markers. Such cells, according to the study, differentiate into cementoblast-like cells, adipocytes and collagen-forming cells. Our previous in vitro studies have clarified that FGF-2 facilitates proliferation while maintaining the differentiation of human periodontal ligament cells (HPDLs). In addition, we now know that the protein does not just stimulate angiogenesis, an action indispensable in the regeneration of tissue, but also increases the production of various types of extracellular matrix from HPDLs [21,35–37]. In short, FGF-2 creates a local environment suitable for the regeneration of periodontal tissue through the activities described above, as part of the mechanism by which regeneration of periodontal tissue is stimulated.

In our clinical trial, to identify adverse events from FGF-2 administered to a particular region of periodontal tissue, we conducted an interview and visual inspection to check the whole body of the patient, checked oral cavity findings and performed clinical inspection. No relationships were identified between